NUMERICAL AND EXPERIMENTAL ANALYSIS OF WAKE EFFECT ON TIDAL CURRENT TURBINE

MUHAMMAD SHAHRUL BIN SABRI

Report submitted in partial fulfillment of requirements
for the award of Bachelor of Mechanical Engineering

FACULTY OF MECHANICAL ENGINEERING
UNIVERSITY OF MALAYSIA PAHANG

JULY 2013

EXAMINER'S DECLARATION

I certify that the project entitled *"Numerical and Experimental Analysis of Wake Effect on Tidal Current Turbine"* is written by *Muhammad Shahrul Sabri*. I have examined the final copy of this report and in my opinion, it is fully adequate in terms of the language standard and report formatting requirement for the award of the degree of Bachelor of Engineering. I herewith recommend that it be accepted in partial fulfillment of the requirements for the degree of Bachelor of Mechanical Engineering.

AZIM BIN MOHD ARSHAD

Examiner   Signature

SUPERVISOR'S DECLARATION

I hereby declare that I have checked this project and in my opinion, this project is adequate in terms of scope and quality for the award of the degree of Bachelor of Mechanical Engineering.

Signature	: …………………………….
Name of Supervisor	: DR. RIZALMAN MAMAT
Position	: ASSOCIATE PROFESSOR
Date	: 11 JULY 2013

STUDENT’S DECLARATION

I hereby declare that the work in this project is my own except for quotations and summaries, which have been duly acknowledged. The project has not been accepted for any degree and is not concurrently submitted for award of other degree.

Signature : …………………………….
Name : MUHAMMAD SHAHRUL BIN SABRI
ID Number : MA09020
Date : 11 JULY 2013

ACKNOWLEDGEMENT

I wish to express my gratitude to the Faculty of Mechanical Engineering (FKM) of University Malaysia Pahang for giving me the chance to do this final year project. Also who supports the financing of my project.

I am extremely grateful to my main supervisor, Dr Rizalman Mamat for his effort guiding me to complete this study. For his constant moral support, valuable advice and encouragement for this study.

A special grateful to the second supervisor, Mr Amir Bin Aziz, which with his help and advice makes this project easier. He taught everything he can so that I can finish this project.

To my friend Nurfaeza and Loh Chong Sean, this two person has been a very cooperative member. Thank you for the relentless discussion that has been very helpful for us to complete our study. In addition, their knowledge has helped me to understand my project thoroughly.

ABSTRACT

The tidal current energy is one of the renewable energy existed on earth. Malaysia has the potential to develop a technology which can utilize this energy to generate electricity. The installation of marine current turbine array requires a deep research to maximize the potential energy of the sea current. Numerical and experimental investigation of tidal current energy extraction has been conducted in this study. Using commercial computational fluid dynamics (CFD) code ANSYS, the lab scale water flume was simulated. For the numerical model, tidal current turbine are represented by an actuator disk instead of scaled down turbine. The actuator disk produces a pressure drop which can be used to calculate the thrust coefficient. The turbulence kinetic energy and the velocity are closely monitored to investigate the wake effect produce. For experimental investigation, a 1m long, 0.2m high and 0.3m width of water channel fabricated. The same parameter which is velocity and turbulence effect downstream are closely monitored thus comparing the result with numerical simulation. Flowmeter is used to read the velocity of the current in the water channel. The result shown wake recover up to 70% at 4D for every numerical and experimental investigation.

ABSTRAK

Tenaga arus laut adalah salah satu tenaga boleh diperbaharui yang wujud di muka bumi. Malaysia mempunyai potensi untuk membangunkan teknologi yang boleh menggunakan tenaga ini untuk menjana elektrik. Pemasangan susunan turbin marin yang boleh mengekstrak tenaga arus laut memerlukan penyelidikan yang mendalam untuk memaksimumkan penjanaan tenaga arus laut. Penyiasatan berangka dan percubaan pasang surut pengeluaran tenaga semasa telah dijalankan dalam kajian ini. Menggunakan dinamik bendalir pengiraan komersial (CFD) ANSYS kod, makmal skala flum air telah disimulasi. Bagi model berangka, turbin air diwakili oleh cakera penggerak bukannya turbin yang telah dikecilkan. Penggerak cakera hasil kejatuhan tekanan yang boleh digunakan untuk mengira pekali teras. Tenaga kinetik dan pergolakan halaju yang memantau untuk mengkaji kesan ekoran yang dihasilkan. Untuk siasatan ujikaji, salurasn air telah diperbuat dengan ukuran 1m panjang, 0.3m lebar, dan 0.2m tinggi. Parameter sama iaitu halaju dan kesan hiliran pergolakan yang dipantau itu dibandingkan hasilnya dengan simulasi berangka. Flowmeter digunakan untuk membaca halaju semasa dalam saluran air. Hasilnya ditunjukkan arus air kembali semula sehingga 70% pada 4D bagi setiap siasatan berangka dan eksperimen.

TABLE OF CONTENTS

LIST OF FIGURES

LIST OF TABLES

LIST OF ABBREVIATIONS

RE	Renewable Energy
MCT	Marine Current Turbine
RTT	Rotach Tidal Turbine
POM	Princeton Ocean Model
EES	Engineering Equation Solver
TPXO	OSU TOPEX/POSEIDON Crossover

CHAPTER 1

INTRODUCTION

1.1 INTRODUCTION

Tidal energy is a form of energy created when the natural rise and fall of ocean surface happen. It is caused by the gravitational field of the sun and the moon. There are two ways the tidal energy can be turned to electricity which is by using tidal barrage and tidal stream approach. Although tidal barrage may develop in Malaysia but it is not economically viable due to high construction cost [1]. There are many countries has been used the tidal energy to generate electricity. France and South Korea are the leader in this hydropower technology. The La Rance and Lake Sinhwa are the respective tidal power station for both countries.

The tidal stream however can be a good source of renewable energy for Malaysia because Malaysia has a few locations with high tidal stream energy [1]. This tidal stream energy can be utilized to become the main energy resource to generate electricity in Malaysia one day. If the tidal energy become the main energy resource of Malaysia it may be able to overcome problems due to the low resource of natural gas and oil.

To achieve this mission, a very deep and thorough research need to be done and more knowledge need to be acquired. There are only very few research has been made lately. This thesis is to increase knowledge of tidal energy in Malaysia.

1.2 PROBLEM STATEMENT

Most of the country nowadays has an awareness of available renewable energy resources. People know that at one time, the energy cannot be generated by non renewable energy resources like coal or natural gas anymore. The world however has a really large of renewable resource. It includes biomass energy, wind energy, solar energy and hydropower energy. This available resources can be utilized to its greatest potential and can be the main energy use which generate the world electricity someday.

Malaysia, the front leader of developing country are going towards the utilization of renewable energy. Tidal is one of renewable energy resource in Malaysia. According to reference [2], Malaysia has thirty nine units of mini hydro with total capacity of 16.185 MW in Peninsular Malaysia, seven units of total capacity of 2.35 MW in Sabah and 5 MW in Sarawak. However the value is still small and further research and development need to be established to enhance this renewable energy.

1.3 RESEARCH OBJECTIVES

Around the world, the marine current energy converter is located in a compact site where the tidal current are constrained such as between the islands, around headlands or estuarine-type inlets [3]. The tidal turbine then needs to be installed in an array so that it is cost efficient. Since the water current possesses a different flow characteristic than the wind, the understanding of the wake effect needs to be researched so that the performance of a tidal turbine array can be kept at its highest. This study aims to understand the effect of wake from tidal turbine within a set of data obtained in a Malaysian sea.

1.4 SCOPE OF THE STUDY

1. Data obtain on tidal current in Malaysia.
2. Actuator disk use as a scale down turbine.
3. Analysis the wake effect using numerical method.
4. Experimental investigation in water channel.
5. Data analysis by comparing numerical and experimental investigation.

CHAPTER 2

LITERATURE REVIEW

2.1 INTRODUCTION

The ocean energy are from four different resources which are wind, tidal, thermal or marine currents. This energy can be used as large scale sustainable electrical power[4]. Although the wind energy is more common resources developed [4], it should not be the only one resources to be focused.The tidal current especially has a very large capacity of energy and can be utilised to be use as renewable energy. Tidal currents have its potential for the generation of renewable energy [5].

Globally, tidal energy is estimated at 2.5 TW of potential power [6]. Hydropower is the only renewable energy source that can boast a substantial share of today's electricity generation [7]. On 2007, hydropower energy share amount of 17% corresponding to total energy supply of EU [8]. Futhermore, this energy has no critical impact to the environment [9]. It is known that there are a few problems regarding to the fish survive and its habitat [10]. However it can be overcome by increasing hatchery of any type fish endangered [11].

As for Malaysia, the potential energy from the ocean are thermal energy, tidal energy and wave energy. The ocean thermal energy required 20°C in the difference between warm sea surface and cold water seabed. The 1000 meters of depth are required to produce the temperature difference. However, Malaysia ocean is only around 50 to 200meters.

East of Sabah ocean however has the required depth but it is 200 to 300 km from its shoreline. The high cost of development needs to be invested to harvest this energy. For the wave energy, Malaysia ocean has only 0.5 to 1.5 meters height. The energy that can be produced is only 15kW per meter. This is too small to meet such high demand. The tidal current however require a minimum speed of 2.5 m s speed. Most Malaysia oceans averagely have 0.77m/s of current speed. The max speed of currents is around 1m/s to 1.2m/s. With a highly research turbine, this potential tidal current energy can be harvested to become the source of energy for Malaysia [12].

2.2 TIDAL FORMATION AND HISTORY

2.1.2 Tidal energy background

The formation of tidal happens when the earth rotates within the moon and sun gravitational fields [13]. Tides usually has three basic patterns, a half day (semi diurnal), daily (diurnal) and a 14-day cycle. A diurnal is cause by the rotation of earth position within the moon gravitational field resulting a 12 hour 25 minutes high level waters. Moreover, the diurnal tides have only one high and low tide within 24 hours. The 14 day cycle is caused by the superposition between moon and sun gravitational field. This formation is shown in figure 1.1.**.**

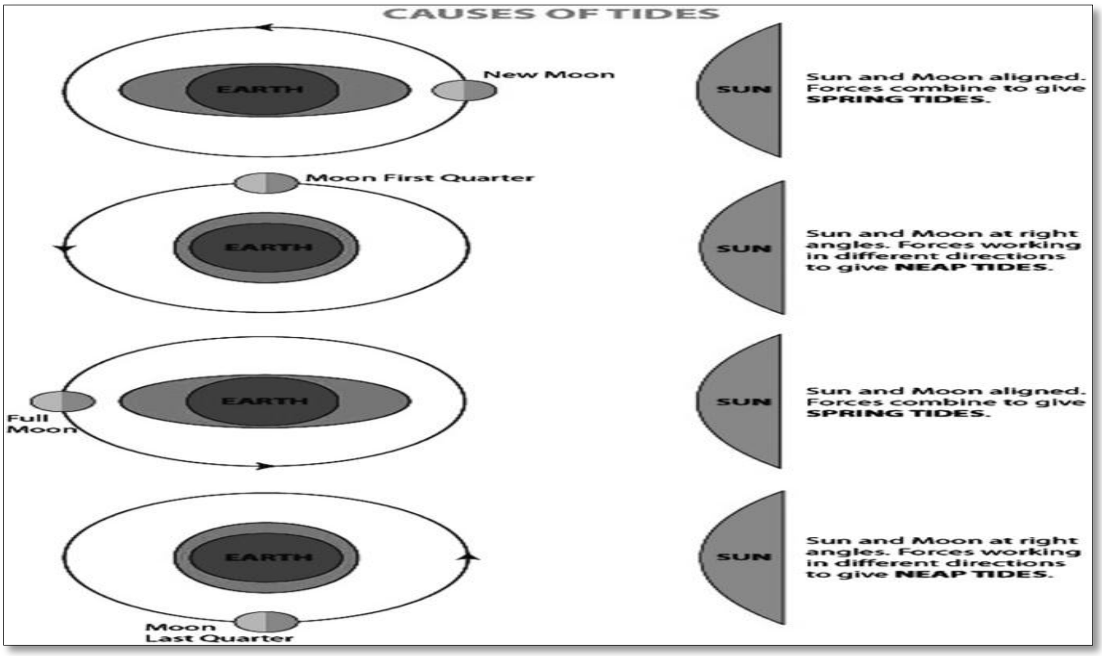

Figure 2.1: Formation of tidal.

Source: X. Sun (2008)

As the tidal formation can be predicted, this renewable energy can be very reliable compared to wind, thermal or wave energy. Hence, the tidal current energy can develop to its full potential [14]. The tidal current application has been used since a long time ago. The earliest date estimated is on 6th century located at Kiloteran near Waterford. It is the first vertical wheel tide mill.

Basically, two types of method use generate electricity from tidal movement [15]. The first method is by building a tidal barrage across an estuary or bay in high tides. This method manipulates the difference between high and low tides. However this method has a very high investment and also environmental issues [16]. Figure 1.2 shows the mechanical work of tidal barrage.

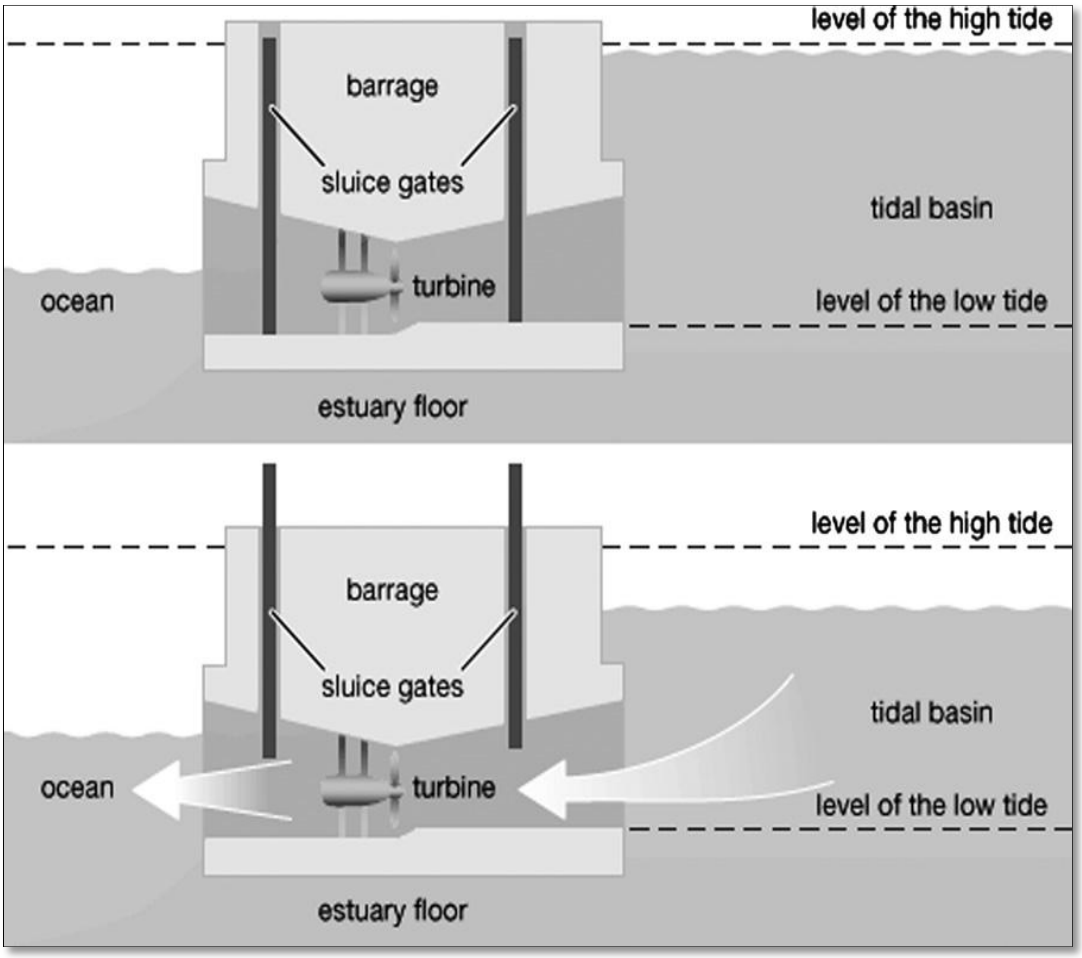

Figure 1.2: Tidal barrage fundamental.

Source: X. Sun (2008)

The most famous tidal barrage is on La Rance, France. It was open on 26th November 1966 and becoming the second largest tidal power station in the world. Currently generated by 24 turbines and can supply up to 240 Megawatts at its peak rate. In addition, it supplies 0.012% of France power demand [17]. It is located on the Severn Estuary between Cardiff and Bristol.

Figure 2.2: La Rance Tidal Power Station

Source: X.Sun (2008)

Figure 2.3: Location of LA Rance Tidal Power Station.

The second method is to build a tidal farm energy extractor. The kinetic energy of flowing water is transferred to electrical energy by energy converter [13]. The converter usually uses to capture the current is tidal current turbine. It applies the same concept as the wind turbine where the kinetic energy converts to electrical energy [18]. This technology also has less impact to the environment also it is deployed under the sea hence reduce the land use [5].

As for Malaysia, tidal energy is a promising renewable energy resource available [19]. A study by Ref [20] identified that Pulau Jambangan, Kota Belud and Sibu are the location with promising for tidal energy extraction. The estimated amount of electricity that can be generated at those three locations is about 14.5 GWh/year [19].

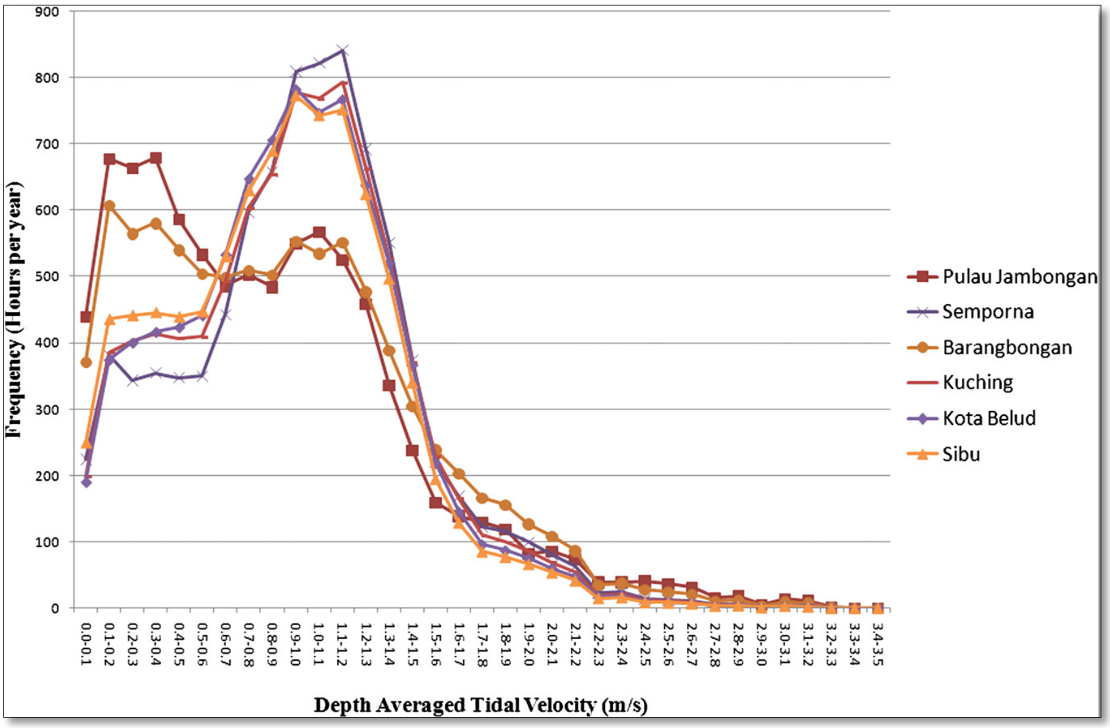

Figure 2.4: Distribution of tidal currents for Sabah and Sarawak.

Source: Y.S Lim (2009)

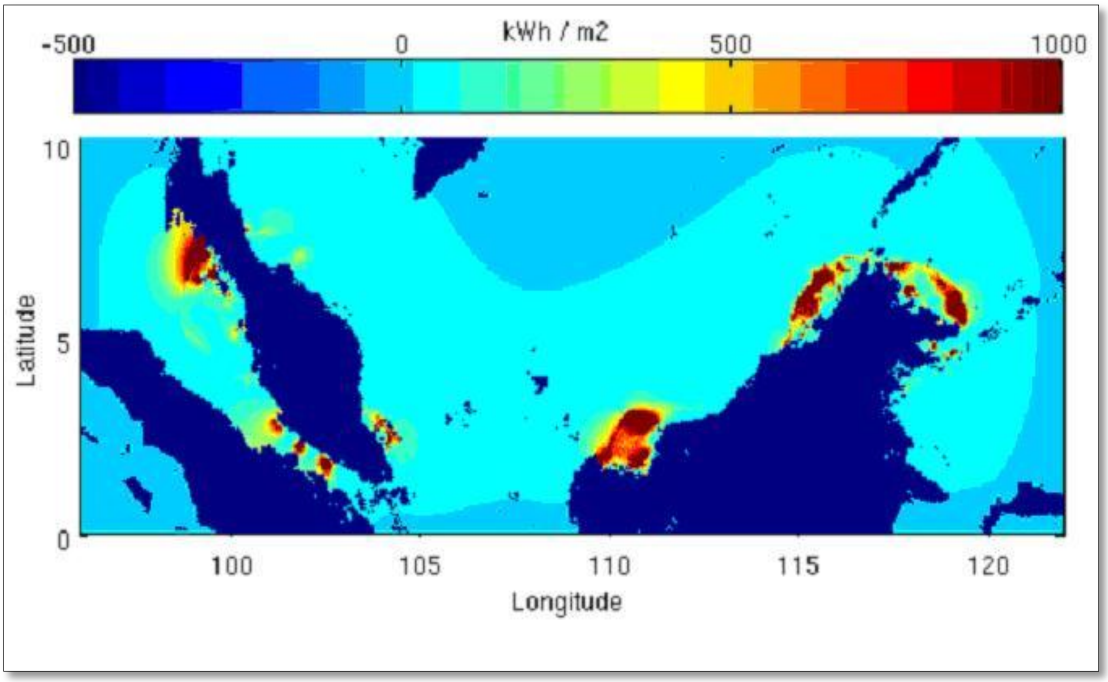

Figure 2.5: Energy density of tidal current in Malaysia.

Source: Y.S Lim (2009)

2.2.2 Tidal energy requirement

The tidal energy available is massive but still in most areas there is too low current speed which is not exceeding 2m/s [13]. The table below shows the relative power density of marine currents with wind and solar resource.

Table 2.1: Relative power density of marine currents with wind and solar resource**.**

Energy resource	**Tidal Currents**					**Wind**	**Solar**
Velocity (m/s)	1	1.5	2	2.5	3	13	Peak at noon
Velocity (Knots)	1.9	2.9	3.9	4.9	5.8	25.3	Peak at noon
Power density (kWm)	0.52	1.74	4.12	8.05	13.91	1.37	~1.0
Note: 13 m/s is a typical velocity at which maximum power is achieved for a wind turbine							

Source: X. Sun (2008)

Other criteria which need to be considered for the requirement to install the turbine is water depth. At 15 m depth at low tide minimum is ideal for 10 m rotor in diameter, at high tide, the height is 50 m at maximum [13]. The table below shows the suggested criteria for horizontal axis tidal current turbine rotor diameter.

Table 2.2: Influence of water depth on maximum permitted turbine.

Water depth	**Rotor diameter (assuming no shipping conclusion)**	**Rotor diameter (assuming shipping exclusion)**
<20m		10m
20-25m	5m	120m
25-40m	10m	20m
>40m	20m	20m

Source: X. Sun (2008)

Malaysia, the country which has large areas of sea, has places where marine current turbines can be installed. According to Y.S Lim [1], three places which has the potential extractable energy is Pulau Jambongan, Kota belud, and Sibu. Below are the table develop using the Princeton Ocean Model (POM) by him.

Table 2.3: Locations and the corresponding potential energy output of an MCEC array, assuming that the power coefficient Cp = 0.4 and the minimum operating current speed is 1.1 m/s.

Locations	**Extractable energy (kWh/m^2/year)**	**Nominal depth**	**Rotor dameter**	**Number of MCTs that can be installed on the site**	**Total swept area (km^2)**	**Energy output (GWh/year)**
Pulau Jabongan	50.16	33	18	50 x 50	0.6	30
Kota Belud	1153.27	93	60	50 x 50	7.1	8188
Sibu	644.60	53	30	30 x 30	0.6	386
Total (GWh/Year)						8604

Source : Y.S. Lim (2009)

In addition, if three of this location utilized this tidal energy, 10% of 83,300 GWh/year of electricity demand in Malaysia will be generated by marine current turbine (MCT) [1].

2.2.3 Types of tidal curent energy extractor

There are numerous number of marine current turbines develop from now. Basically there are two types of tidal current energy extractor. This is the most common use of turbine types.

1. Horizontal axis turbine
2. Vertical axis turbine
3. Variable foil systems
4. Venturi systems

The horizontal axis turbine extracts energy the same way as the wind turbine extract energy from moving air [15]. It works when the inflow perpendicular to the rotor causes a resultant hydrodynamic force, which has components acting normal to the axis of the rotor blade in the plane of rotation [13]. The resulting torque is transferred by a shaft and gearbox to an electrical generator [21].

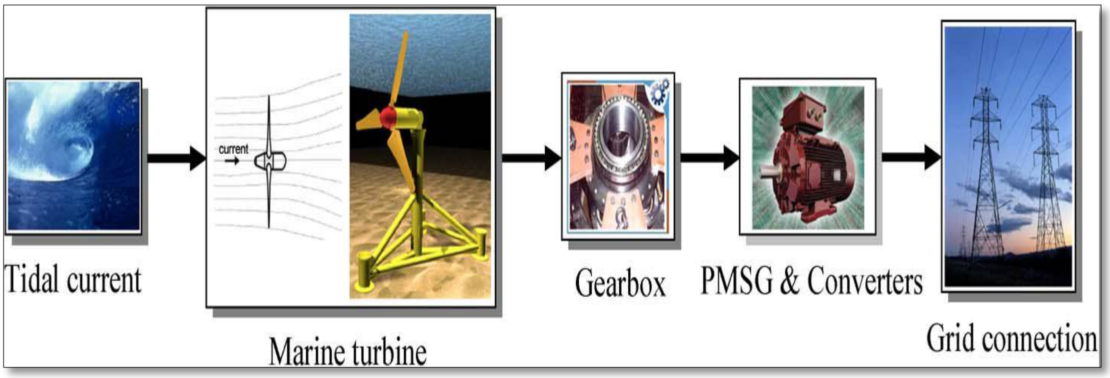

Figure 2.6: Marine current turbine global block diagram.

Source: Benelghali (2011)

The most successful example of a horizontal axis turbine is the Seaflow developed by Marine Current Turbine Ltd. In 2003, MCT in association with Seacore successfully installed the 300kW Seaflow in the Bristol Channel near Lynmouth, United Kingdom [22].

Figure 2.7: Marine Current Turbine Seaflow

Source: Benelghali (2011)

For the vertical axis turbine, the blades and rotor transmission shaft are parallel to one another and are both oriented perpendicular to the incoming current flow [13]. Two types of vertical axis turbine are Savonius type and Darrieus type. The Savonius type is a drag type and the Darrius type apply a lift type.

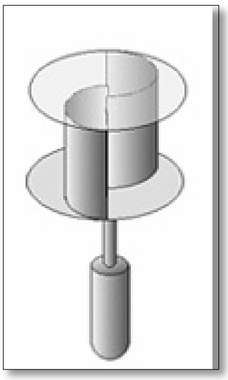

Figure 2.8: Savonius type.

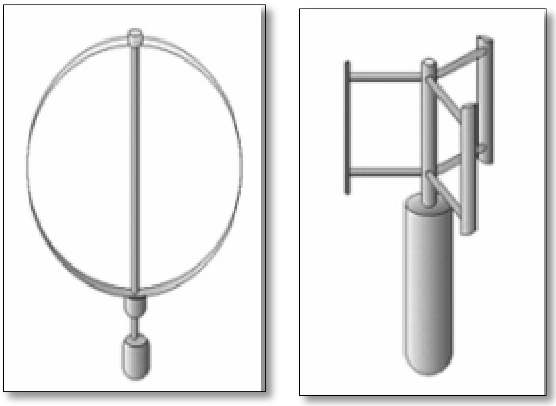

Figure 2.9: Darrieus type.

In addition, current research has been made so that both of the advantages of these two type of vertical axis turbine can be combined. The hybrid vertical axis turbine has many advantages including flexibility to meet specified design criteria, simple in structure and easy to build [23]. The figure below shows the hybrid model of the vertical axis turbine.

Figure 2.10: Hybrid model.

The 'Stingray' develops by Engineering Business Ltd is the most famous variable file systems types energy extractor. In September 2002, Stingray was installed at Yell Sound in UK for the testing period. The 250kW rated demonstrator produced 250kW at peak capacity and averaged 90kW in a 1.5 m/s measured current during its initial power cycles [14]. The Stingray has the supporting arm part which will oscillate when the stream of the sea flow through it thus forcing the hydraulic cylinders to extend and retract. This movement produced high-pressure oil that used to drive a generator [24].

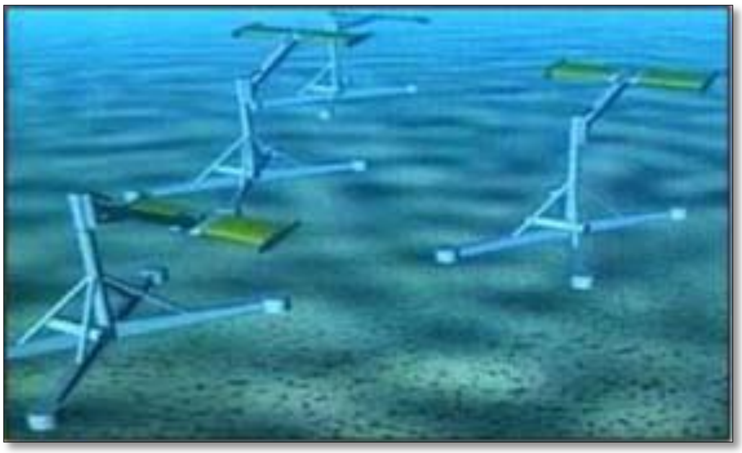

Figure 2.11: Artist impression of Stingray array on seabed.

Lastly, the Venturi systems applies the Bernoulli principle. The system reduces the pressure by accelerating the primary flow passes through the device. The pressure drops cause the current flow nearby sucked into it. This sucked flow is used to drive the onshore turbine and generate electricity. Below are the figure of Venturi system turbine develop by Lunar Energy.

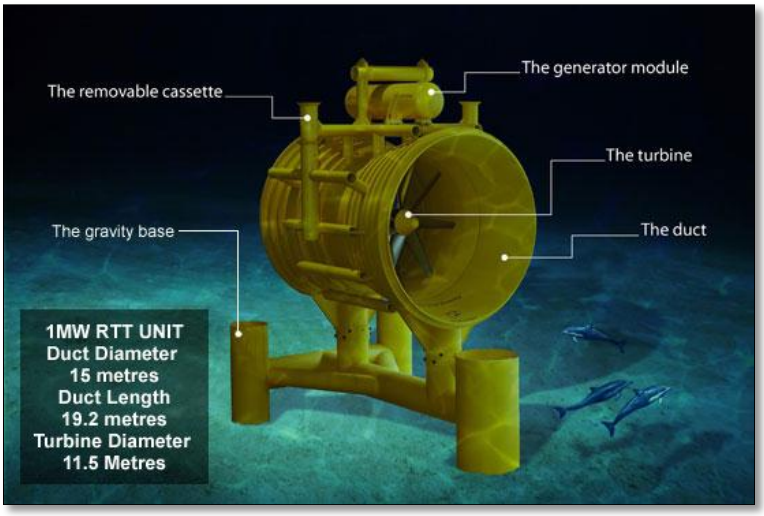

Figure 2.12: Rotach Tidal turbine by Lunar Energy [25]

Source: Lunar Energy. Co. UK

In addition, according to the reference [26] tidal turbine may seem similar to modern wind turbine however,the design of tidal turbine array may be appreciably different, predominantly due to :

- Decreased lateral spacing (perpendicular to flow). Many sites with strong tidal flows have a bi-directional flow characteristic, thus the lateral spacing of devices could be reduced. However, there will be a limit to this spacing to prevent detrimental downstream wake interactions
- Staggered or increased row spacing. Devices will need to be located far enough downstream to ensure that both the free stream flow velocity is recovered and that turbulence is not excessive.
- Proximity to flow boundaries. Rotors are expected to sweep close to the sea bed and the water surface in a fluid that typically may only be twice the rotor diameter in height.

CHAPTER 3

METHODOLOGY

3.1 NON-DIMENSIONAL SCALING

Most of studies predicting the power characteristics for tidal stream turbine have assumed an idealized water flow with a uniform velocity profile such in the figure below. However, in real sea condition, the actual velocity profile may be different and it is important to understand the model scale performance characteristics can be scaled to account not only for different water velocities and turbine sizes but to also account for a non-uniform velocity profile [27].

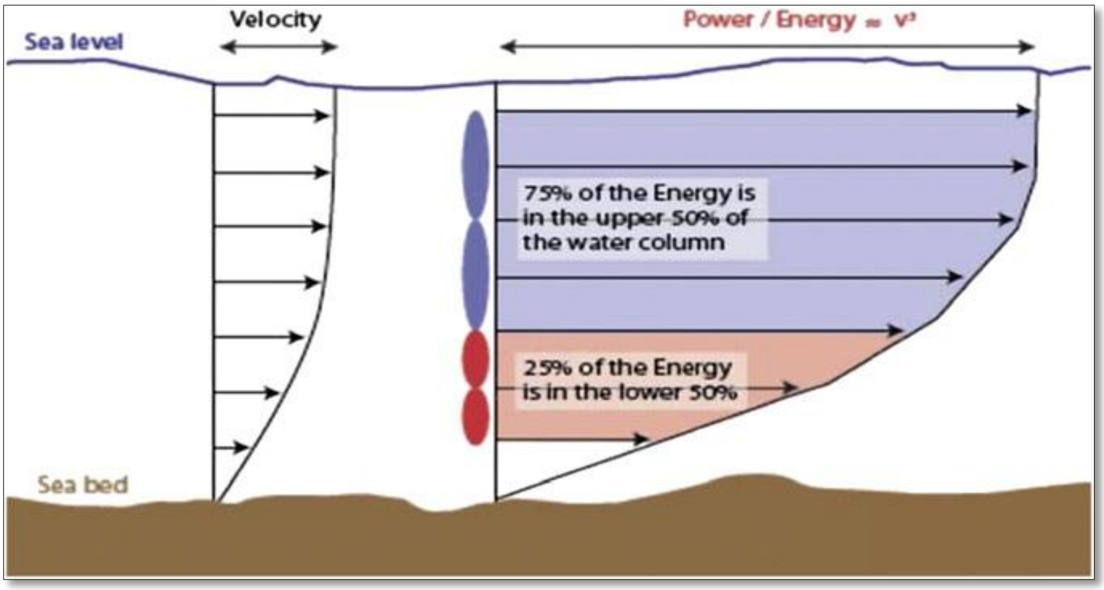

Figure 13: Velocity and power distribution through water column [27].

Source: A. Mason Jones (2012)

3.1.1 Turbulence Modelling

The turbulent flow occurs when the Reynold's number Re > 2000 for open channel flow. The fluid will behave randomly at this higher Reynold number. At lower Reynold number, Re < 500 for open channel flow, the fluid is laminar and behave smoothly in a parallel layer without interruption.

Given,

$$\mathrm{Re} = \frac{\rho UL}{\mu} \qquad (2.6)$$

Where,

ρ = density of fluid

U = free stream fluid velocity

L = characteristic length scale of the flow

μ = dynamic viscosity of fluid.

For open channel flow:

Re < 500 (laminar flow)

Re > 2000 (turbulent flow)

3.1.2 Froude Theorem

The Froude theorem is a representation of sea water condition in a water channel by considering the inertia and gravity effect of the water flow. It uses to scale down the sea condition in a water channel. The same Froude number will give the same expected velocity profile in a sea.

$$Fr = \frac{V}{\sqrt{gl}} \qquad (2.21)$$

Where,

V = velocity of water

g = gravitational force

l = depth of the water from bottom

Where the number of froude represents the flow characteristic of water.

Fr = 1 (critical flow)

Fr < 1 (subcritical flow)

Fr > 1 (super critical flow)

3.1.3 Coefficient of Thrust

Most of the first generation of MCT will have difference thrust according to the power which will be generated. For scaling issue of tidal turbine to actuator disk, the generated thrust need to be in same to predict the wake behavior. The thrust of the actuator disk can be control of the level of porosity made.

$$C_t = \frac{\Delta P}{0.5\rho U^2} \tag{2.22}$$

$$C_t = \frac{T}{0.5\rho U^2 A} \tag{2.23}$$

Where,

ΔP = pressure difference

ρ = density of fluid involve

A = area of porous disk

T = force on the porous disk

U = initial velocity of water

3.2 NUMERICAL MODELLING

3.2.1 Computational Fluid Dynamics

Computerized dynamic is a numerical approach to solve and analyze the fluid flow problem with computer technology. This software is very dependent on the computer performance which includes a central processing unit (CPU) and storage capacity. This software helps to simulate the complicated fluid flow phenomena which cannot be seen by experimental setup. CFD also may give an earlier estimations before experimenters started. This may save cost and time efficiency.

Nowadays, this CFD software is used by many people in the area of fluid dynamics. There are three steps in every CFD simulation which is :

1. Preprocessing
2. Solver
3. Post process

Preprocessing step

Preprocessing is the first step in CFD simulations. It is used to define the geometry of the flow model to solve. The computational grid is also built at this stage. The computer aided design software such as solidwork or AutoCAD can be used to build this computational grid. Basically, there are structured and unstructured grid that can be generated based on the flow domain. For structured grid, the grid is in regular rows and column. Furthermore, the unstructured grid cells are in an irregular pattern. CFD accuracy is very dependant upon the number of cells in its computational grid. In this stage, fluid properties and the conditions along the boundary of solution domain also must be set.

Solver

At this stage, CFD runs the flow calculation and obtain numerical results by solving governing equations. Discretization of the governing equations is an important part at this stage. Basically, three methods of discretizing the governing equations which are finite difference, finite volume and finite element. For the finite volume method, the solution domain needs to be divided into a finite number of contagious control volume (CVs) which is small volumes surrounding each node point in the grid. Node point is the centroid of a CV. Moreover, the differential form of the governing equations is integrated over each CV. This method is a conservative method because it defines that fluxes such as mass, momentum, energy and species entering a given CV is identical to the fluxes leaving the adjacent CV. In addition, this method can be used for any type of grids including complex geometries. For the finite element method are formed by combining the nodes in predetermined topology. The accuracy of this method depends on the fineness of discretization in that for a finer mesh. This method is at advantages to problems of great complexity and unusual geometry. Lastly, for the finite difference method, the computational domain including the boundary of the physical problem is covered by a grid.

Postprocessing

On postprocessing stage, the numerical results are produced and presented. The most CFD software uses a versatile data visualization functions to generate high resolution CFD images and animations. This is great to interpret the numerical results and understand the flow of the fluid.

3.2.2 Governing Equations of Fluid Flow

In order to show the numerical problems of any fluid flow problem in CFD, a mathematical equation need to be solved first. According to [28], the cornerstone of computational fluid dynamics is the fundamental governing equation of fluid dynamics – the continuity, momentum and energy equations.

Physical principle - mass is conserved

Net mass flow out of CV = time rate of decrease of mass inside CV

Or,

B = C

Where B and C are symbols of left and right respectively.

The continuity equation can be expressed in a Cartesian coordinate system

$$\frac{\partial \rho}{\partial t}+\frac{\partial(\rho u)}{\partial x}+\frac{\partial(\rho v)}{\partial y}+\frac{\partial(\rho w)}{\partial z}=0 \tag{2.1}$$

For an incompressible fluid, the density (p) is constant and equation 2.1 becomes

$$\frac{\partial u}{\partial x}+\frac{\partial v}{\partial y}+\frac{\partial w}{\partial z}=0 \tag{2.2}$$

Since *x* (*i* = 1, 2, 3) represents *x, y, z* coordinates. Furthermore, *u* (*i* = 1, 2, 3) are the velocity components as u, v, w in the i th direction. Therefore, equation 2.2 can be shown as

$$\frac{\partial u}{\partial x}=0 \tag{2.3}$$

Navier-Stokes equations

The Newton's 2nd law expressed F=ma. When applied to the moving fluid element, the net force on the fluid element equals its mass times the acceleration of the element. This is the vector element and can be expressed in scalar relations along *x, y,* and *z* axis.

The x component in the Navier-Stokes equation

$$\rho\left[\frac{\partial u}{\partial t}+u\frac{\partial u}{\partial x}+v\frac{\partial u}{\partial y}+w\frac{\partial u}{\partial z}\right]=\mu\left[\frac{\partial^2 u}{\partial x^2}+\frac{\partial^2 u}{\partial y^2}+\frac{\partial^2 u}{\partial z^2}\right]-\frac{\partial p}{\partial x}+X \tag{2.4a}$$

The y component in the Navier-Stokes equation

$$\rho\left[\frac{\partial v}{\partial t}+u\frac{\partial v}{\partial x}+v\frac{\partial v}{\partial y}+w\frac{\partial v}{\partial z}\right]=\mu\left[\frac{\partial^2 v}{\partial x^2}+\frac{\partial^2 v}{\partial y^2}+\frac{\partial^2 v}{\partial z^2}\right]-\frac{\partial p}{\partial y}+Y \tag{2.4b}$$

The z component in the Navier-Stokes equation

$$\rho\left[\frac{\partial w}{\partial t}+u\frac{\partial w}{\partial x}+v\frac{\partial w}{\partial y}+w\frac{\partial w}{\partial z}\right]=\mu\left[\frac{\partial^2 w}{\partial x^2}+\frac{\partial^2 w}{\partial y^2}+\frac{\partial^2 w}{\partial z^2}\right]-\frac{\partial p}{\partial z}+Z \tag{2.4c}$$

Where,

ρ = density of fluid

p = pressure

μ = dynamic viscosity of fluid

u, v, and *w* denotes velocity components in the *x, y, z* component,

and *X, Y*, and *Z* are the body force

The left side represents the total accelerations in the three directions. On the right side represent resultant forces acting on the fluid particle. Oftenly, the Navier-Stokes equation are written as

$$\rho\frac{\partial u}{\partial t}+\rho u\frac{\partial u}{\partial x}=\mu\frac{\partial^2 u}{\partial x\partial x}-\frac{\partial p}{\partial x}+X \tag{2.5}$$

Where *X* is a body force per unit volume in the *i* th direction.

3.2.3 Free Surface Modelling

Free surface is the interface between two immiscible fluids such as water and air. The free surface is not fixed and it may vary both spatially and temporally. This free surface is difficult to be encountered in this CFD modelling.

Sometimes, the rigid lid approximation is used and the free surface are treated as an imaginary frictionless horizontal plane on which the velocity perpendicular to the plane is zero and the velocity tangential to the plane is non – zero. This type of approach saves time but its only restricted under the hypothesis that there are no significant variations in the water free surface.

The numerical methods of free surface can be grouped into two categories, moving grid method and fix grid method.

Moving a grid method and fix grid method

In this method, the free surface is considered as the boundary if a surface fitted grid and the computational grid is permitted to move with the free surface. By doing this method, free surface can be precisely computed. However, in dealing with complex 3D free surface geometry this method can be very difficult and time consuming.

On the other hand, the fix grid methods use the fixed stationary computational grid that covers both gas and liquid and can be divided into two cases which is a surface capturing method and surface tracking method. The free surface tracking method exploits the position of the free surface where it is explicitly distinguished. It also allows tracking by the pre-defined markers that can be a scalar function. This method allows the governing equation only in the liquid and the free surface grid cells to be solved. For the surface capturing method, it avoids the need for the complicated free surface tracking process by regarding the free surface as a discontinuity in a density field and being captured automatically in the computation of gas-liquid flow. The surface-capturing allow the governing equations solved simultaneously for both gas and liquid regions.

The Volume of Fluid method (VOF) is used in modelling of free surfaces. The VOF method considers two or more fluids that are not interpenetrating each other. Every phase is represented by their own volume fraction in every grid cell and the volume fractions of all phases in one control volume fraction in each cell. For the water and air interface, air is defined as the primary phase and its volume fraction is denoted by a_1. Water is defined as secondary phase and volume fraction can be denoted as a_2. In control volume there exist three possible conditions for water volume fraction a_2:

$a_2 = 0$:	the cell is empty (of water but full of air)
$a_2=1$:	the cell is full (of water but empty of air)
$0 < a_2 < 1$	the cell contains the interface between air and water.

In order to calculate the volume fraction of air a_2, the following equation used.

$$\frac{\partial a_1}{\partial t} + u\frac{\partial a_2}{\partial x} = 0 \qquad (2.16)$$

In order to calculate the volume fraction of air a_1, the following equation used.

$$a_1 = 1 - a_2 \tag{2.17}$$

Therefore, the interface is known in every control volume.

The following equations determine the fluid properties like density and dynamic viscosity by a1 and a2 in each control volume.

$$\rho = a_1\rho_1 + a_2\rho_2 \tag{2.18}$$

$$\mu = a_1\mu_1 + a_2\mu_2 \tag{2.19}$$

Where,

μ_1 = air dynamic viscosity

μ_2 = water dynamic viscosity

ρ_1 = air density

ρ_2 = water density

The equation below are a single momentum equation.

$$\rho\frac{\partial ui}{\partial t} + \rho\frac{\partial(uiuf)}{\partial xf} = -\frac{\partial p}{\partial xi} + \frac{\partial}{\partial xf}\mu\left(\frac{\partial ut}{\partial xf} + \frac{\partial uf}{\partial xi}\right) + \rho gi + Fi \tag{2.20}$$

Where,

ρg_i = gravitational body force

F_i = external body force

3.2.4 Actuator Disk Theory

The actuator disk theory has been used to simulate wind turbine since Froude formulated it. This actuator disk theory is easy to implement especially is used with RANS (Reynold Average Navier Stokes) solution and the standard k-ε turbulence model and may give under predictions of the wake effects that is larger in the near wake region [29, 30].

A streamtube enclosing the turbine rotor is considered. The rotor is simulated as a semi permeable disc with the same diameter and placed perpendicular to the direction of flow. A uniform pressure jump created by the flow passing through this semi permeable disc are a represented load on the real rotor. The inflow and outflow boundaries of the streamtube are taken far from the actuator disk, where undisturbed atmospheric pressure already formed and the flow velocity is considered uniform at each cross section of the tube.

This actuator disk theory is commonly used in the wind turbine concept. However it is acceptable to the current turbine since it is valid for any fluid. Much research for propeller and tidal current turbine simulation has used this theory [13].

3.2.5 Numerical Methods

By establishing all the mathematical equations, a discretization method needs to be chosen. Discretization is a method of approximating the differential equations by a system if algebraic equations for the variables at some set of discrete locations in space and time [31]. Three common discretization approach is available which is a finite difference (FD), finite volume (FV) and finite element (FE).

In FV, value of the flow variables at the surface of one control volume need to be obtained in terms of the centroid values of its neighboring cell face by using the suitable interpolation scheme.

Numerical Solution Methods Properties

Based on Ferziger and Peric [31] below properties are summarized.

(a) Consistency

A consistent method has a zero truncation error when the grid spacing is equal to zero and/or time step is zero. Truncation error is the difference between the discretized equation and the exact one. Usually, the truncation error is proportional to a power of grid spacing and/or time step. If most or all of important term is proportional to the grid spacing and time step the in the-order approximation must greater than zero to be considered consistence.

(b) Stability

If the numerical solution method does not magnify the errors that appear in the course of the solution process, it is said to be stable. The stability guarantees that the method produces a bounded solution whenever the solution of exact equation is bounded. In addition, for the iterative method, the one that does not diverge is a suitable method.

(c) Convergence

If the solution of the discretized equations tends to the exact solution of the differential equations as the grid spacing tends to zero, it is said the numerical method is convergent. A consistent scheme is useless if the solution method does not converge. For a nonlinear problem, the stability convergence of a method is difficult to be shown. In order to demonstrate this, convergence is checked using numerical experiments.

(d) Conservation

At steady state, the amount of a conserved quantity leaving a closed volume is same as the amount by entering the volume. It is based on the conservation laws. If finite volume method and a strong conservation form of equations is used, this is guaranteed for each individual control volume and for the solution domain as a whole.

(e) Boundedness

For a numerical solution, it must be bounded. For example, a nonnegative quantity like density must always be positive. A concentration must have a value within 0% to 100%.

3.2.6 CFX Setup in Numerical Modelling

(a) Geometry

A round disk is drawn with solid work software with 3mm thickness and 100mm in diameter. 22 hole size of 8mm in diameter is made of symmetrically. The drawing then is saved in igs file type then exported to Ansys CFX modelling. The rectangular enclosure is drawn which have a 100 cm in length, 30 cm in width and 30 cm in height. The test disk is placed in the middle of water depth which is 5cm from the waterbed. The figure below shows the geometry drawn with the disk placed.

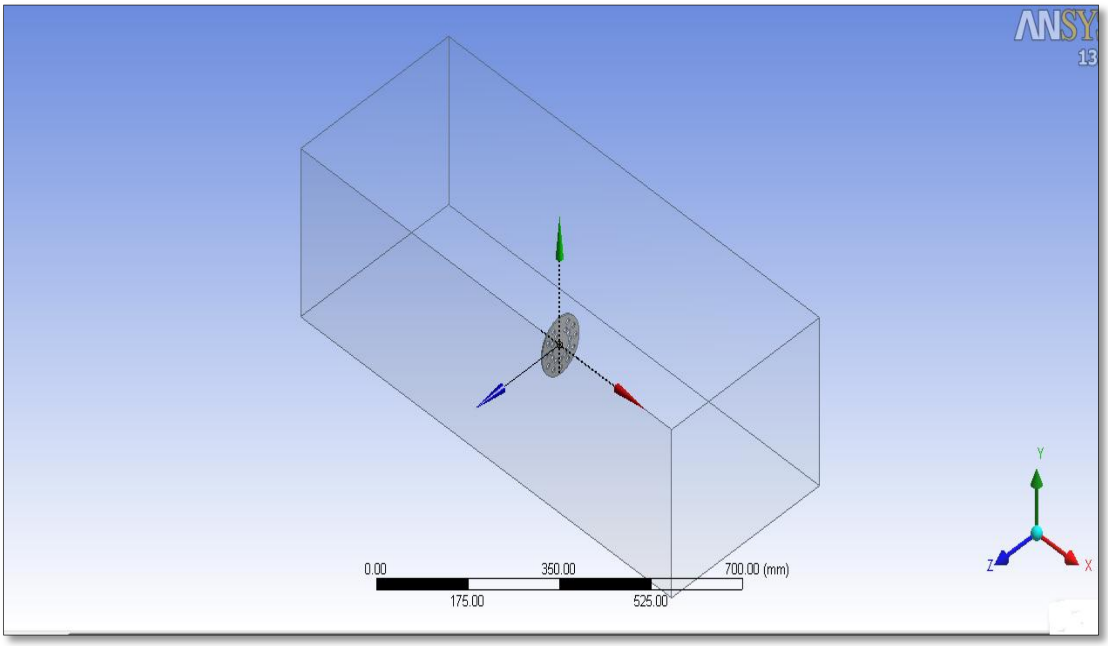

Figure 3.2 : A geometry setup.

(b) Mesh

In this meshing setup, only the size of the mesh is set. The relevance center is set to medium, the smoothing setup is set to medium, the minimum size of mesh is 2.793e-4 meters and the max size is 5.5861e-2 m. This results on 50683 numbers of nodes and 251274 elements. The more nodes involve, the higher the accuracy of result but will take much time to complete. This is the reasonable nodes number in this numerical modelling.

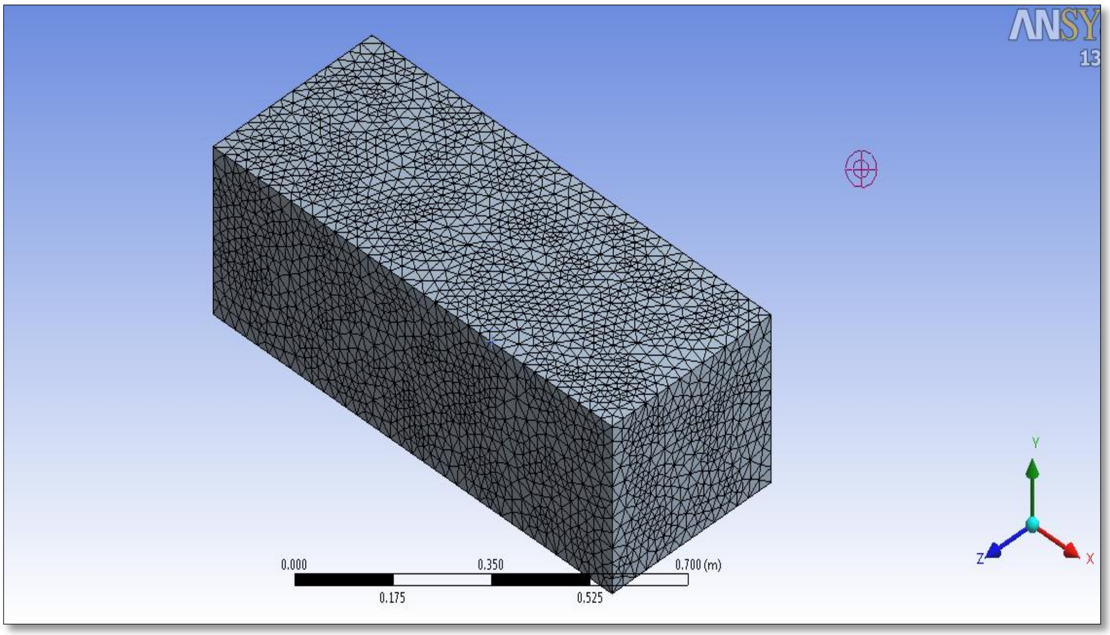

Figure 3.3: Meshing the geometry.

(c) Setup

On the CFX-Pre, the enclosure and the test disk are two different states. The porous disk is set to solid domain and material cost is aluminium The enclosure part is renamed to water channel. The water channel consists of two main element which is air and water. In the fluid models of water channel an SST turbulence option is chosen to increase accuracy.. The inlet of water channel is set to 0.1m/s of inlet velocity. Since this is the open channel type, the upper part is set to open with air volume fraction is 1 while the water volume fraction is 0. The outlet part of water channel is set to static pressure with down pressure in the relative pressure option. As for the body of water channel, the wall is set to no slip wall for mass and momentum and smooth wall for wall roughness.

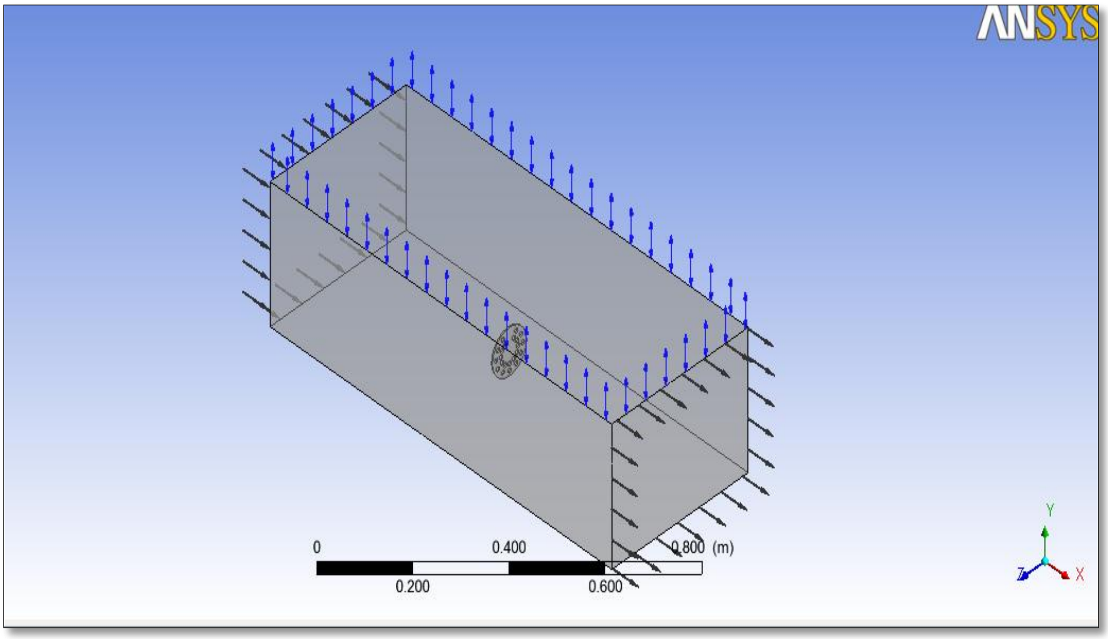

Figure 3.4: CFX-Pre setup.

(d) Solution

The solution control manipulated to get the better result. The timescale control is set to auto timescale with the 1.0 timescale factor. The residual type is set to RMS and residual target is 0.00001.

3.3 EXPERIMENTAL INVESTIGATION

3.3.1 Actuator Disk

A tidal current farm can be very cost efficient to be built because the maintenance can be saved due to the turbine installed in a closed area. The installation cost also will be greatly decreased while the power generated by the farm will be increase depending on the capacity of tidal turbine. However, a wake effect of this tidal turbine should not be neglected. The spacing between each installed turbine may become an influenced factor due to the loss of energy in velocity after each turbine. When the tidal current pass through a turbine, its water velocity will be decreased greatly due to the losses to the turbine blade. After some particular distance, the velocity of the water will be recovered. So this wake distance can be simulated by a turbine simulator. In a small scale lab test channel, the actuator disk used to simulate a real tidal turbine. According to [32], actuator disk most accurately resemble the far wake region. The principle parameters that require accurate scaling to ensure similar behavior in tidal turbine is:

1. The level of disk porosity control to ensure the generated thrust is same as actual turbine.
2. Linear scaling of length ratios such as disk diameter to water depth and channel width.
3. Replication of ambient flow field condition such as Froude number, vertical velocity profile and turbulence intensities. Full scale and model Reynolds number cannot achieve parity at very small scale but should still lie within the turbulent classification.

However, there are a few limitations of using the actuator disk based on M. E. Harrison [33].

1. The porous disc will converts the water current into small scale turbulence instead of extracting the energy.
2. The vortices shed from the edges of the disc is not similar to the bladed turbine.
3. Unlike a rotating blade, the disc will never have a any swirl occur.

The actuator disk is fabricated with a 3mm thick aluminium plate. The diameter of the disk is 100mm. One with 22 holes drilled symmetrically with 8mm in diameter and another one with 35 holes to ensure equal thrust generated. This actuator disk is a scale down of the 10m turbine at 15 RPM. At 10 cm disk, this actuator disk should have a 1500 revolution per minute. However, this condition is not possible with current technology. Thus it is desirable to use an actuator disk to simulate a tidal turbine.

Figure 3.5: Porous disk with 14% porosity.

Figure 3.6: Porous disk with 22% porosity.

3.3.2 Test Disk Support Frame

The support frame designed with an aluminium bracket as a main material. It is mounted on the table with screw fasteners supported with an L shaped bracket to ensure less vibration occur in the test disk. The frame is connected to the triangular bolted aluminium plates. To connect the frame to the actuator disk, a shaft is made with a 300 mm long aluminium which have 3mm thickness and 10 mm wide. The shaft connected to the frame with two holes drilled and mounted on 1mm thickness plate. It is recommended that the hole drill nearly possible to the strain gage position. Another 2 hole drilled and bolted on the disk to tightly hold the disk position. This setup is to ensure that the plate is tight enough and does not influence the strain gage reading.

Figure 3.7: The test disk support frame.

3.3.3 Strain Gauge

Strain gauge used to measure the strain on the shaft connecting the disk and the support bracket. The force on the disk can be measured by calibrating the disk with the initial force tested push pull gauge. A very delicate work of solder should be practiced since the solder area is really small.

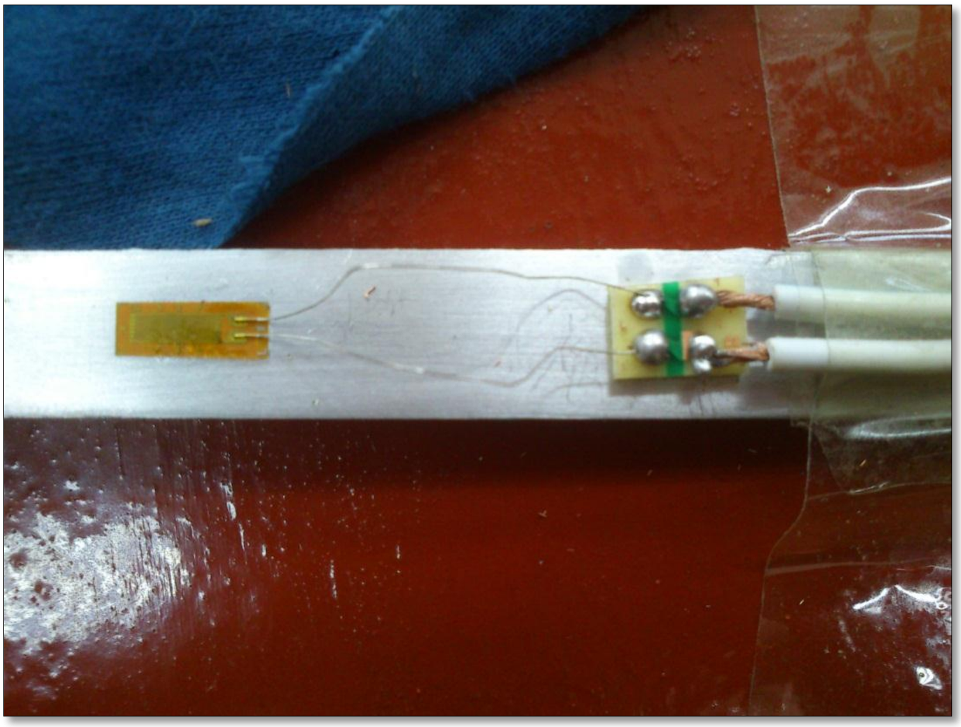

Figure 3.8: Strain gauge on a shaft.

3.3.4 Push-Pull Gauge

The push pull gauge device is used in calibrating the strain gauge. It used to measure the strain at certain load specified at the center of the disk.

Figure 3.9: Push Pull Gauge

3.3.5 Data Acquisition

The data acquisition used for the experiment is from National Instrument model no 9202. The daq will convert the signal received from strain gage to digital number in laptop. The use of this daq only capable to 1.92 Hz of sample reading thus the data obtain is smaller.

Figure 3.10: Data Acquisition Device

3.3.6 Test Section Setup

The disk is mounted on the shaft connected to the support frame. The strain gage placed nearest to the disk location but at a safest distance so that the strain gage does not wet. The data acquisition device placed on the support frame, and safely hold by duct tape. The laptop acquires the data from the data acquisition device connected with wire. A Ni-Max software is used to visualize the data obtain. The Dasy lab software also used to visualized the data accumulated and automatically write to the excel sheet.

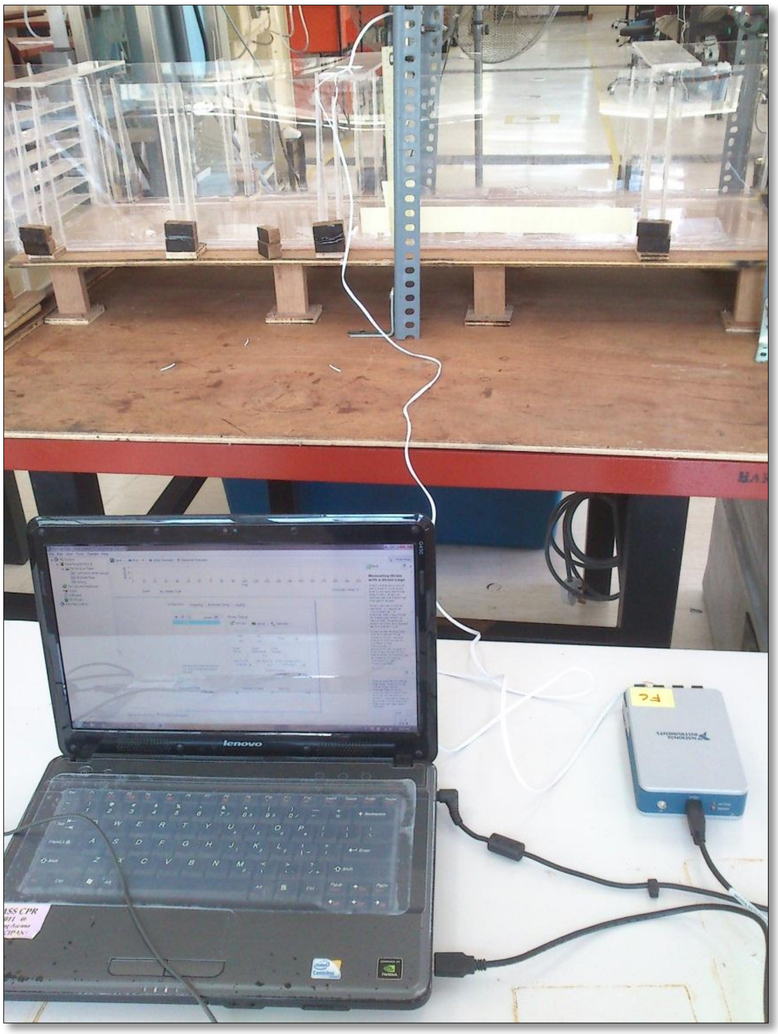

Figure 3.11: Experiment setup.

3.3.7 Flow Meter

Flow meter used to measure the velocity of water at different layers. This device is important to validate the numerical result predicted before. The flowmeter must be the type which can be submerged under water.

Figure 3.12: Flow meter.

3.3.8 Water Channel

The water channel is the most important part of this study since the water in the channel will simulate the real sea water current condition. It has taken up to 11 weeks to finish fabricating the water channel. Many problems encountered however the water channel is finished within the time allocated. A 2hp pump used to pump the water in the channel.. The main frame is a 1cm thick of acrylic glass. The water runs in a 10 cm in diameter pipe. The water velocity control of a ball valve. The water is supplied from a $1m^3$ tank.

Figure 3.13: Water channel.

3.3.9 Experimental Procedures

a. The thrust coefficient experiment.

The experiment held on May 2013 as the water channel is just recently finished completely. The test channel assembled a day earlier. The first step is to ensure that the water velocity is 0.1m/s. The pump is turned on and the water flow through the water channel. The ball valve initially set at half opening and the water volume flow rate is manually obtained. The volume flow rate of water is obtained by simple experiment which a water at a certain level in the basin fill in a few second. The time recorded and the water volume flow rate converted to the water velocity. It's about three times the procedure cycled until the desire water flow rate obtained. The second step is to do a calibration test on the strain gage. To obtain the strain gage calibration data, the disk is initially set at rest without any water in the test section. The 0N load is recorded on the excel sheet. Then, the force applied to the plate from 0.5N until 2N. On every each force applied, the strain gage reading recorded on the excel sheet. Due to manually hold the push pull gauge, only 10 readings with less error selected and the average of each reading calculated. Then the graph is made to produce a linear function which will be used to calculate the drag force coefficient of 0.1 m/s water velocity. After the calibration graph obtained, the pump is turned on and the water level is kept at 20 cm in height which can be manually adjusted by the lever. After a few moments, the data is recorded and can be viewed on the excel sheet. 10 readings are selected and the average of the reading calculated. The reading then compared to the calibration graph obtained. A calibration test and the experiment were run a few times until reasonable data obtain. The figure below shows the calibrated graph for strain gage.

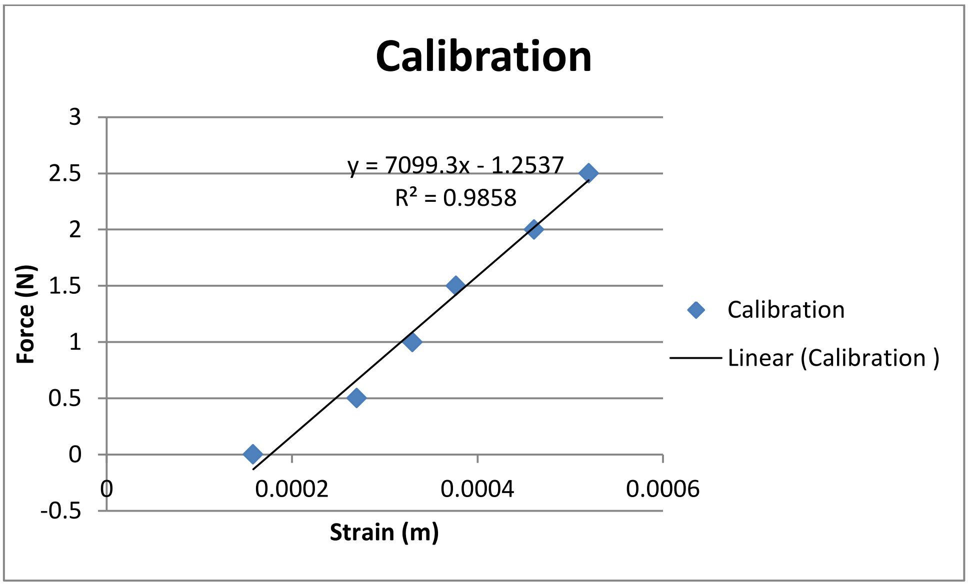

Figure 3.14: Calibration graph for strain gage.

b. The velocity measurement

The experiment of velocity is made to ensure that the behavior of water after the disk is similar to numerical result. This ensures that the wake effect experiment can be done also similar to numerical result. The water velocity is taken in 1D up to 5D downstream. The disk is setup in the same position as the drag coefficient experiment. The water has also run in a similar condition as before. 3 points of interest in diameter of the disk are taken. The velocity of water measured by the flowmeter. This type of flow meter is a blade type and occupy 5cm^2 of the area. So, this causeless point can be measured. The result is being taken and a graph of velocity profile has been made.

c. The wake effect experiment.

This experiment purpose is to visualize the wake effect occur at downstream level. A tape is used to mark the downstream level on the other side of the wall. A white backdrop used to minimize the shadow effect and clearly show the flow of the dye. A camera placed strategically to ensure it captures the effect of dye used. A blue dye used in the experiment as to clearly visualize a water flow around the test disk. After all the equipment set up, the pump is turned on until the water reaches 20 cm height. After a few moments, when the water is steady, a dye is injected using syringe. A blue dye flow behavior was captured by the camera.

3.3.10 Experiment Flow Chart

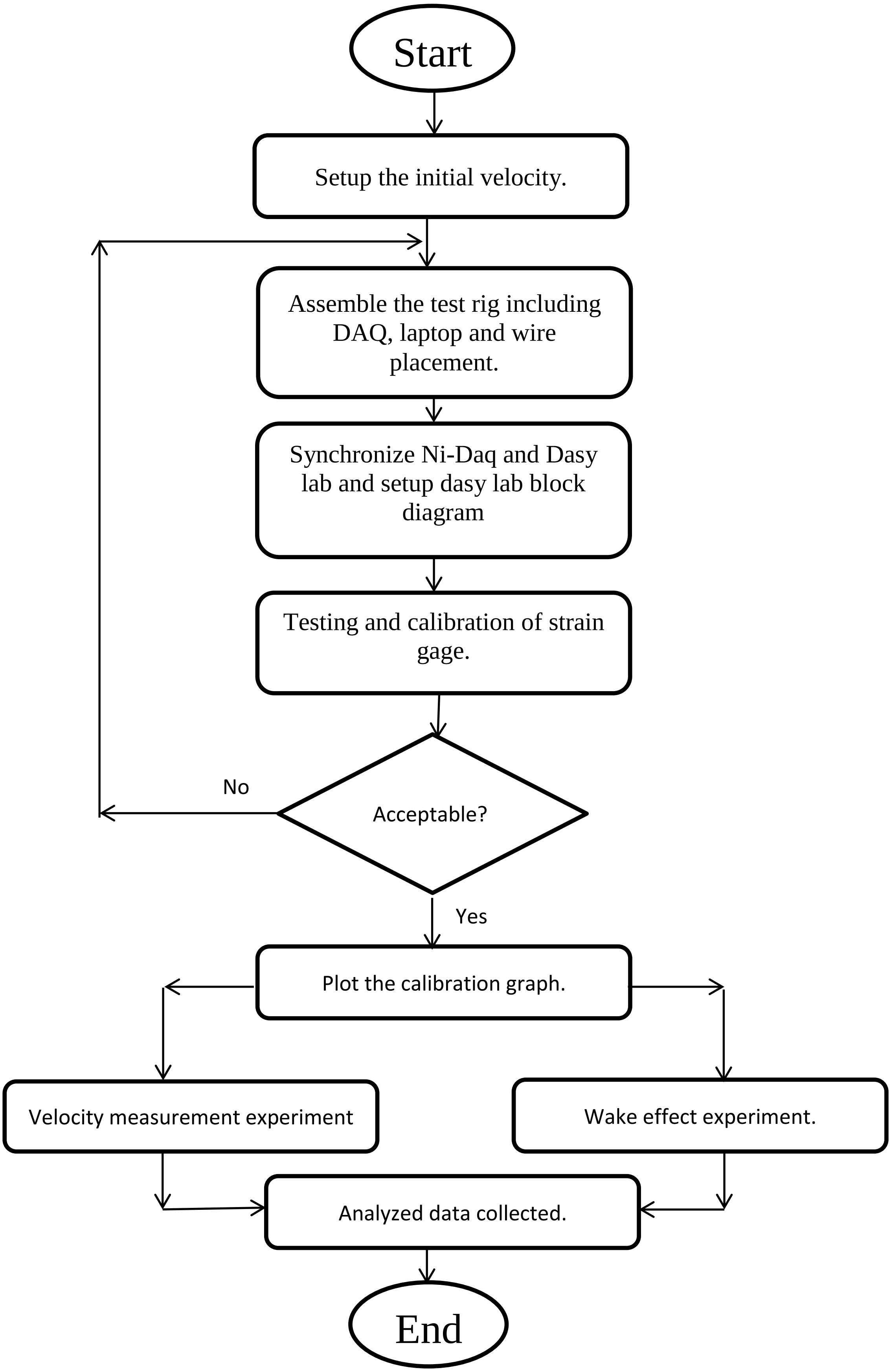

CHAPTER 4

RESULTS AND DISCUSSION

4.1 NUMERICAL MODELLING

By using the Froude number similarity, at 0.1 m/s of water is equal to 1.2 m/s of water in the Sabah sea water according to the data by Y.S Lim [34]. Thus this ensures that the Froude similarity between the water behavior in water channel. The result from numerical simulation using ANSYS-CFX software is shown.

4.1.1 Air Volume Fraction

The air volume fraction is important to make sure that the mixture between air and water is acceptable and logically accepted. The atmospheric pressure should make the water to stay at the bottom. The figure below shows that there are separated boundary between air and water. The water also mixed and resulting in a mixture at between 17cm to 25cm from the bottom of the channel. This is where the boundary that water is wavvy.

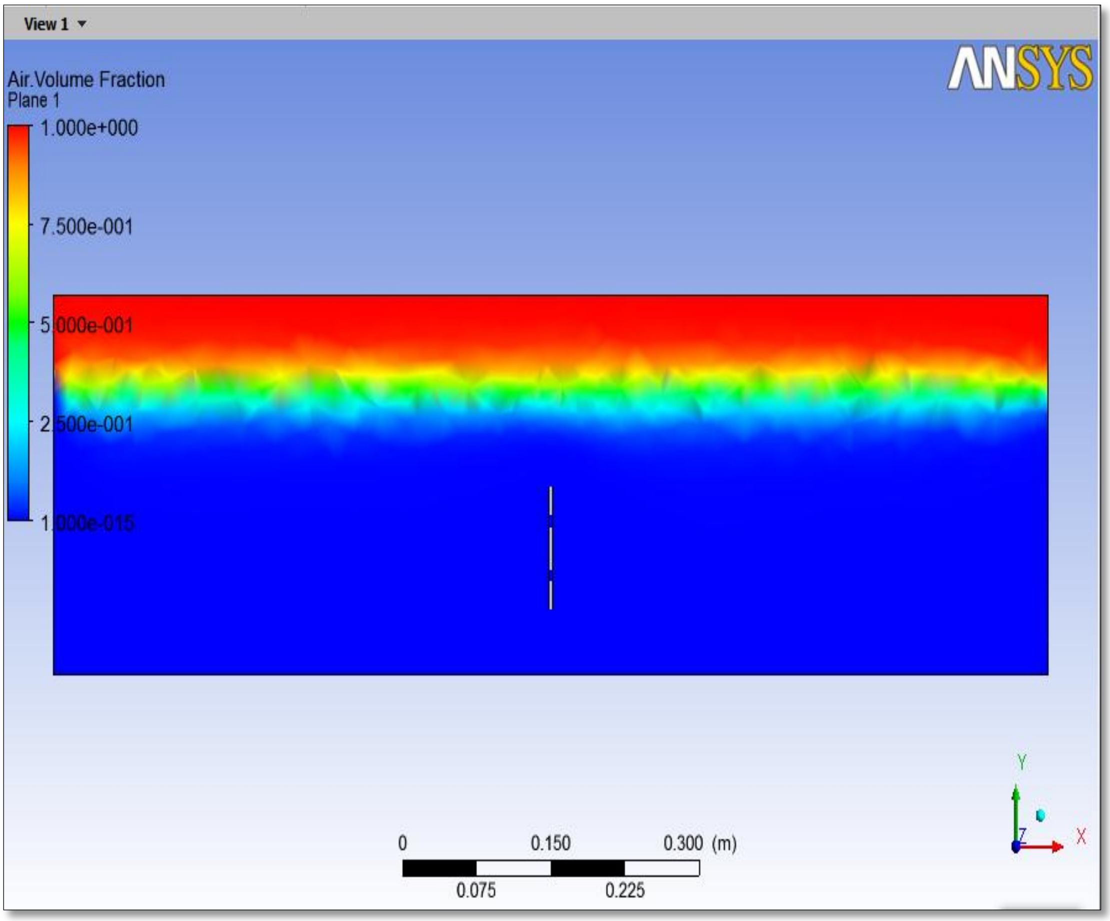

Figure 4.1: Air volume fraction in water channel.

4.1.2 Pressure Drop

The pressure drop is important to measure the coefficient of thrust numerically. From the numerical simulation both of the 14% and 22% porosity disk generated 2.0 and 1.2 coefficient of thrust by using the equation for 2.22. The pressure drop measured across the centerline of the disk.

Table 4.1: Numerical result of thrust coefficient

Porous Disk (%)	Pressure Difference (Pa)	Coefficient of thrust (Ct)
14	10	2.0
22	5.6	1.12

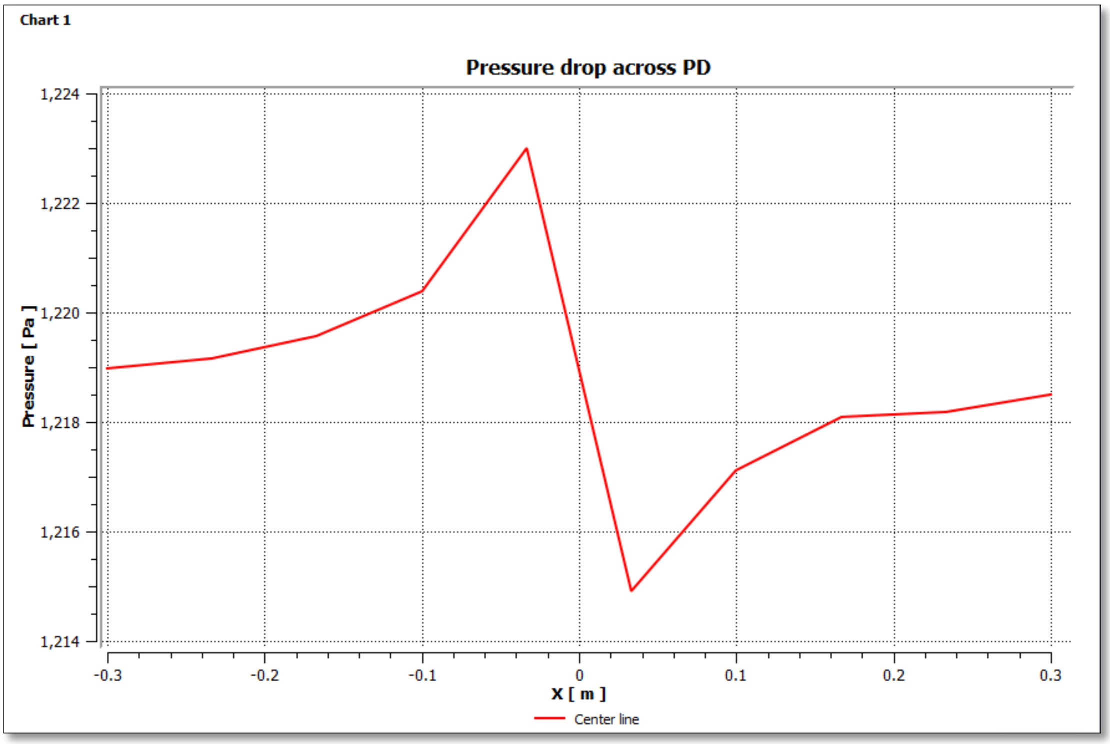

Figure 4.2: Pressure drop across 14% porosity disk.

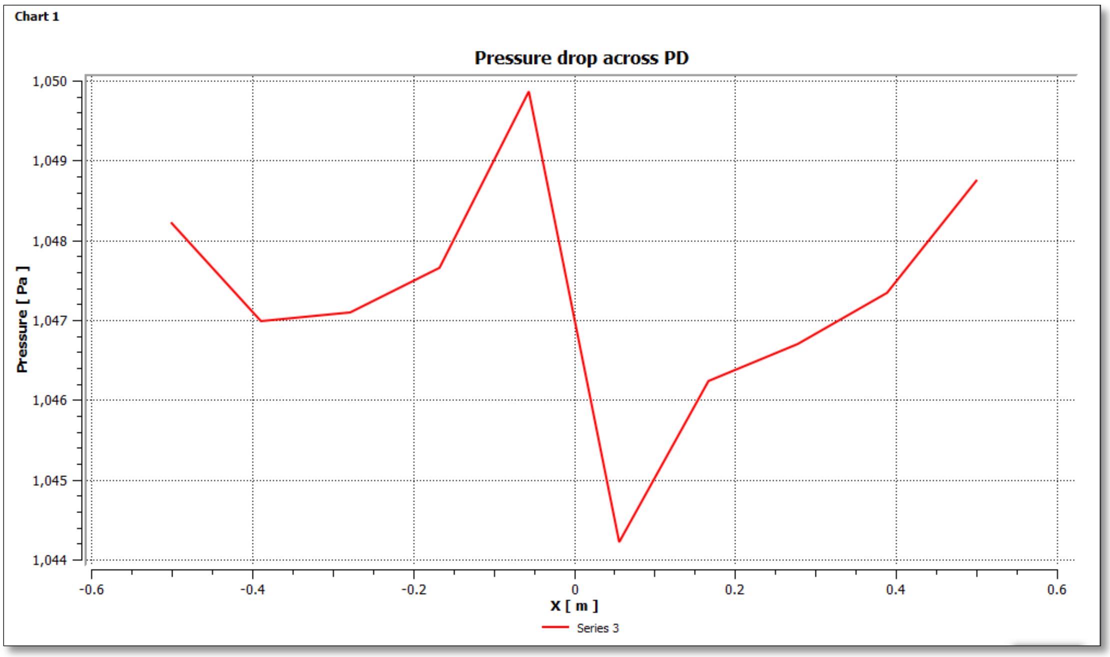

Figure 4.3: Pressure drop across 22% porosity disk.

4.1.3 Velocity Deficit

The velocity deficit use to predict the far wake recovery region. When the velocity is recovering from its initial velocity before it hits the disk the kinetic energy of water is recovered. The figure below shows the velocity profile for both disks at 2D, 3D and 4D downstream.

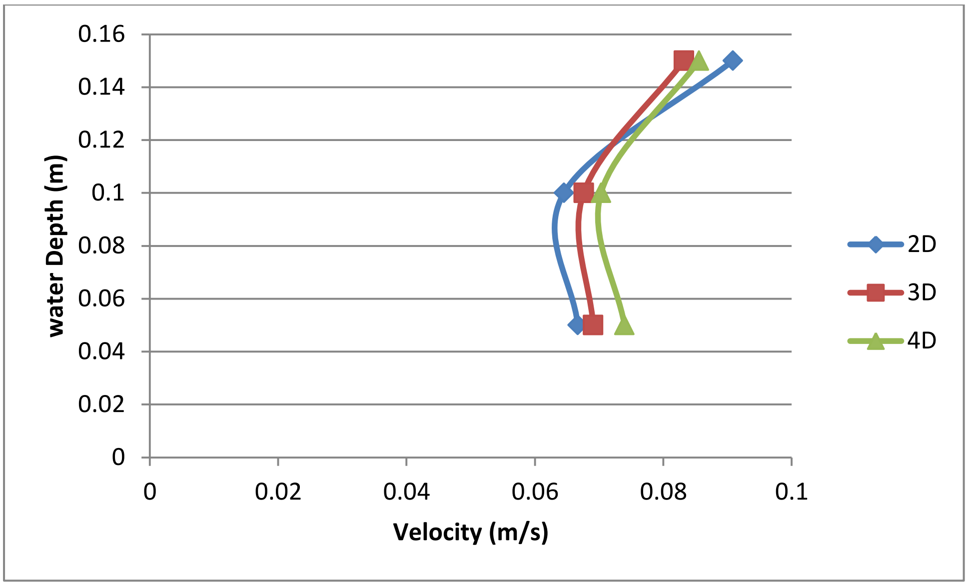

Figure 4.4: Numerical result of 14% porosity velocity deficit.

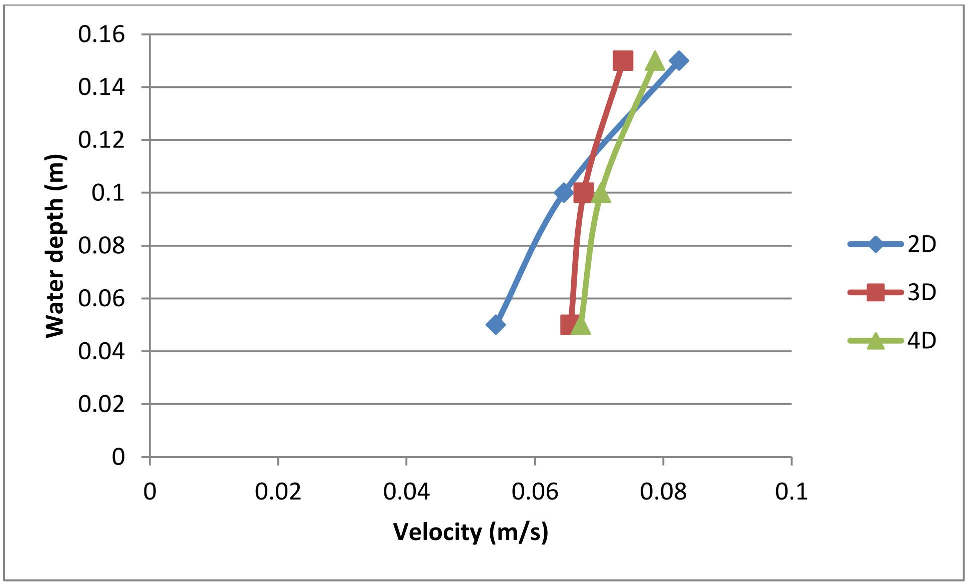

Figure 4,514: Numerical result of 22% porosity velocity deficit.

4.1.4 Turbulence Intensity

The numerical modelling resulting in an almost same condition of turbulence in both 2 disks. Below are the result obtain from the CFD post.

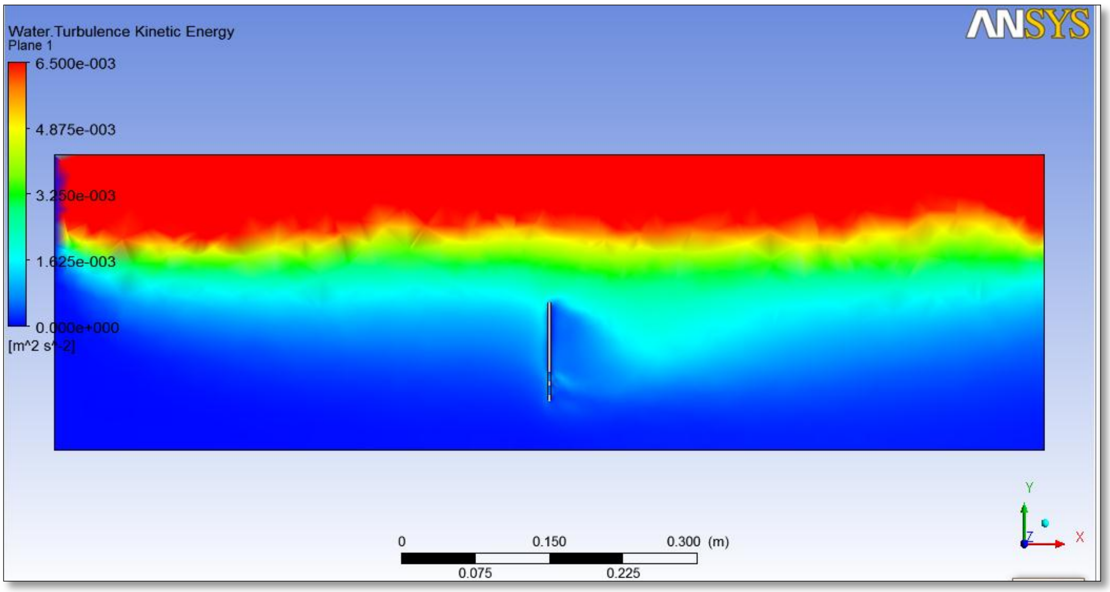

Figure 4.6: Result obtained from 14% disk (side view)

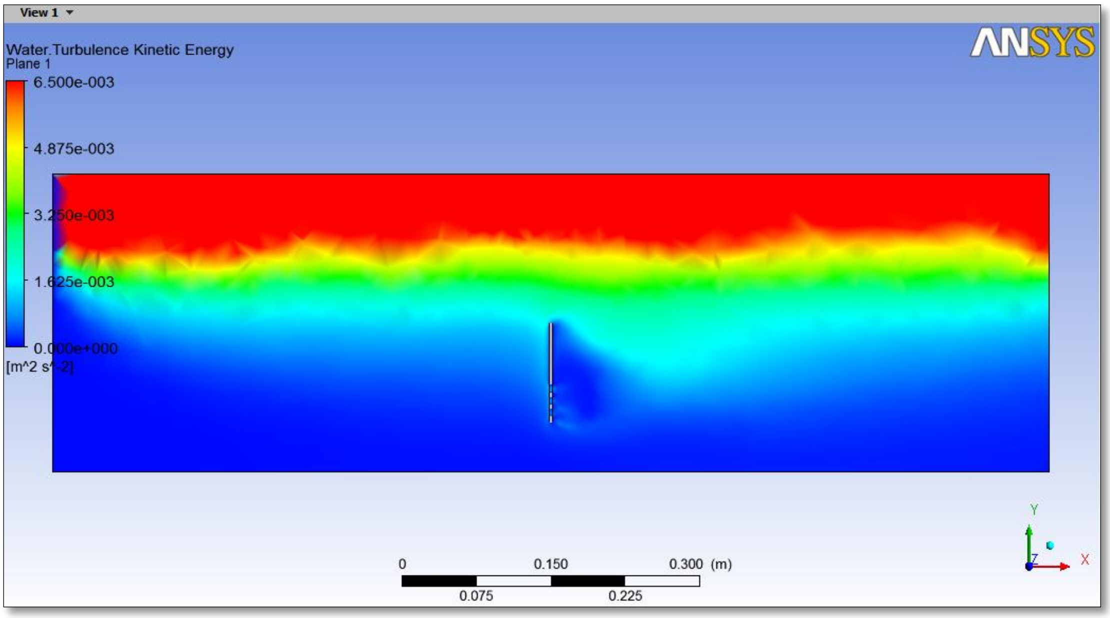

Figure 4.7: Result obtained from 22% disk (side view)

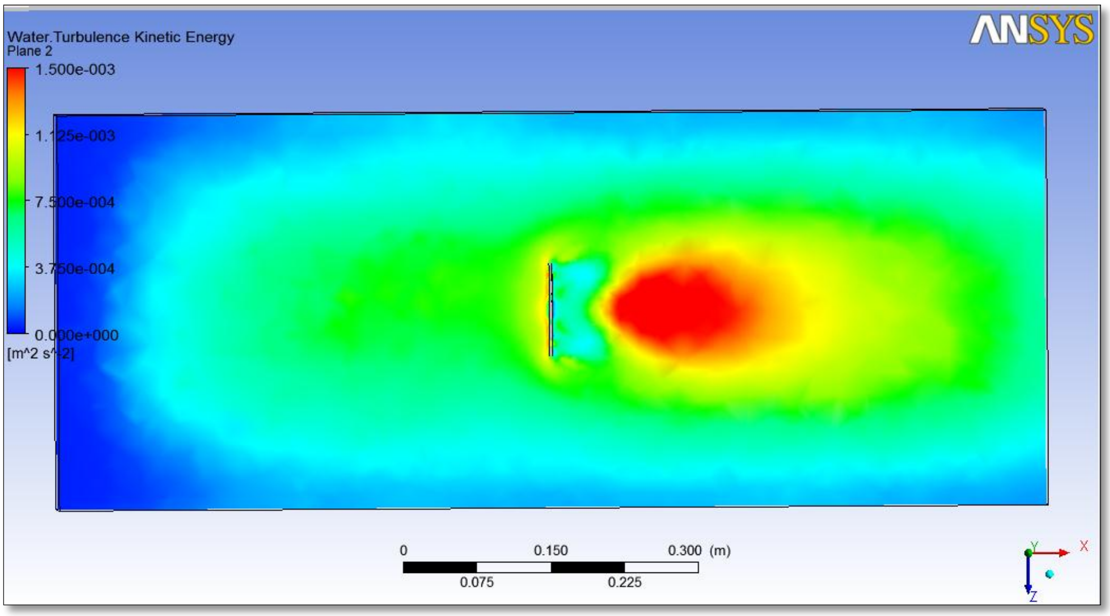

Figure 4.8: Result obtained from 14% disk (up view)

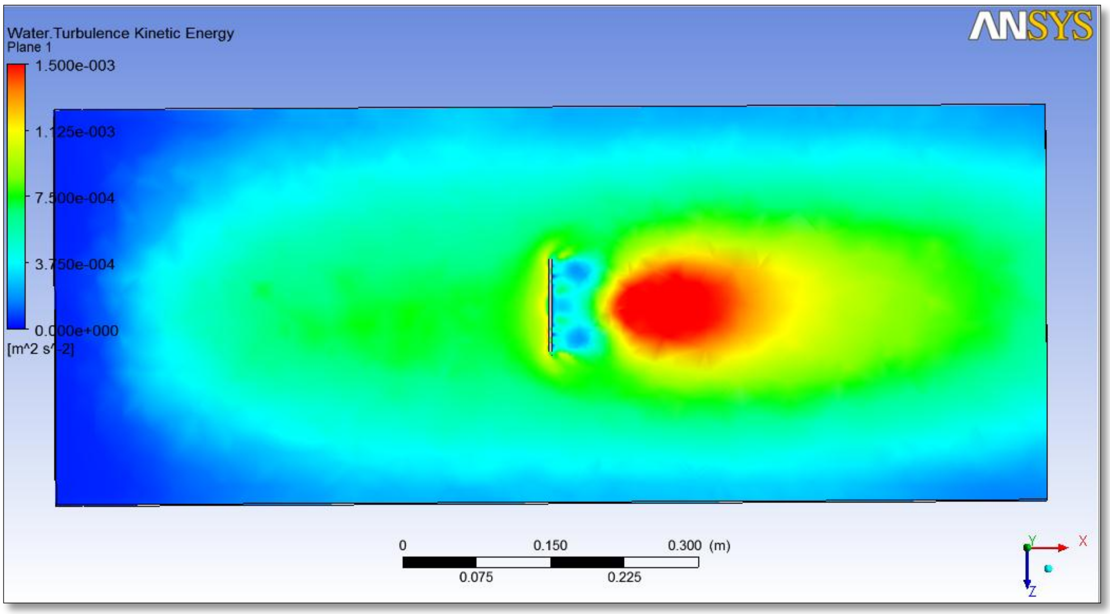

Figure 4.9: Result obtained from 22% disk (up view)

It can be seen that the water turbulence kinetic energy is high around 1D position and getting slower downstream. The high kinetic energy means the turbulence of the water flow is higher. That is the reason there are 0 m/s reading of velocity at 1D position. At 4D the kinetic energy is slower since the water velocity is moving towards the downstream in a steady movement.

4.2 EXPERIMENTAL INVESTIGATION

4.2.1 Coefficient of Thrust

The first experiment resulted in a close approximation to a numerical result value of thrust coefficient. The raw data processed and the average of strain and force is calculated. The table below shows the data obtained from the experiment.

Table 4.2: Experimental result of thrust coefficient

Porous Disk (%)	**Strain**	**Force**	**Coefficient of thrust (Ct)**
14	0.00015464	0.074272	2.2
22	0.00020257	0.011906	1.35

4.2.2 Velocity Deficit

The reading taken from 3 points in a disk region which is along the center, top and bottom of the disk. At 1D position, for experimental investigation, the value of flow meter shows the unsteady reading ranging between 0 m/s to 0.01 m/s of water velocity. This is due to the near wake region where the turbulence kinetic energy of water is highest. Since the flow meter is a blade type, the water kinetic energy will move the blade. However, at 1D, since the turbulence is high, the blade moving too slow thus giving unsteady reading.

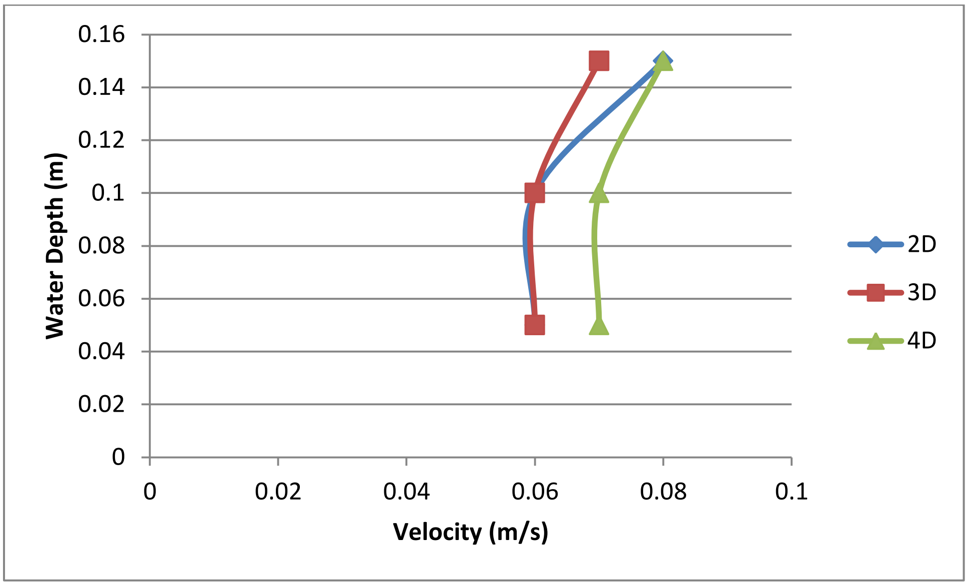

Figure 4.10: Experimental result of 14% porosity velocity deficit

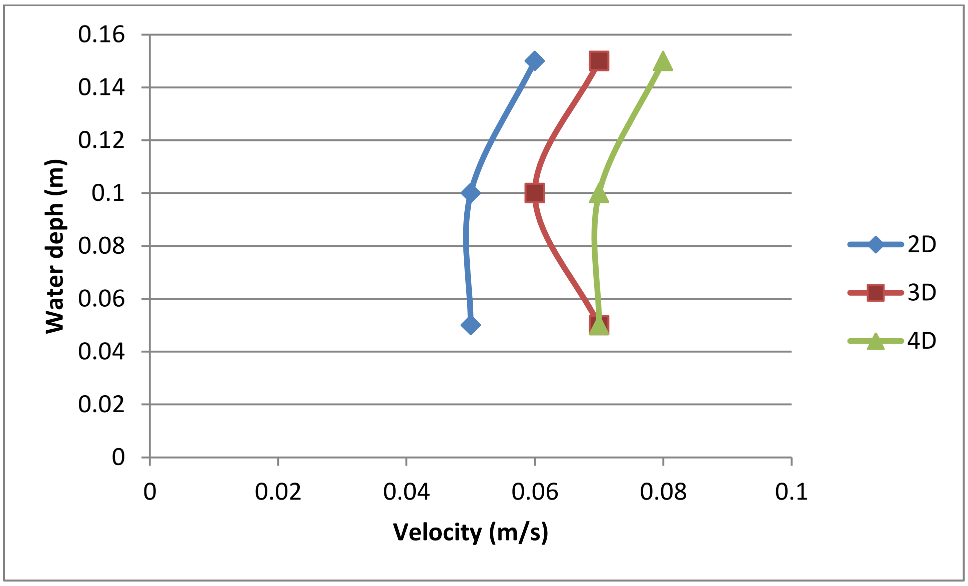

Figure 4.11: Experimental result of 22% porosity velocity deficit

The graph shows that for both numerical and experimental investigations, at 1D position the velocity is at lowest. The increasing in the velocity recovery is getting higher downstream. The velocity is higher at 4D downstream due to the wake recovery from upper and lower region of the disk.

4.2.3 Turbulence Effect

The figure shown the effect of high turbulence at the 1D position as predicted on the numerical simulation. The water is more steady downstream at 2D, 3D, and 4D. The video may give a better visualization of flow effect.

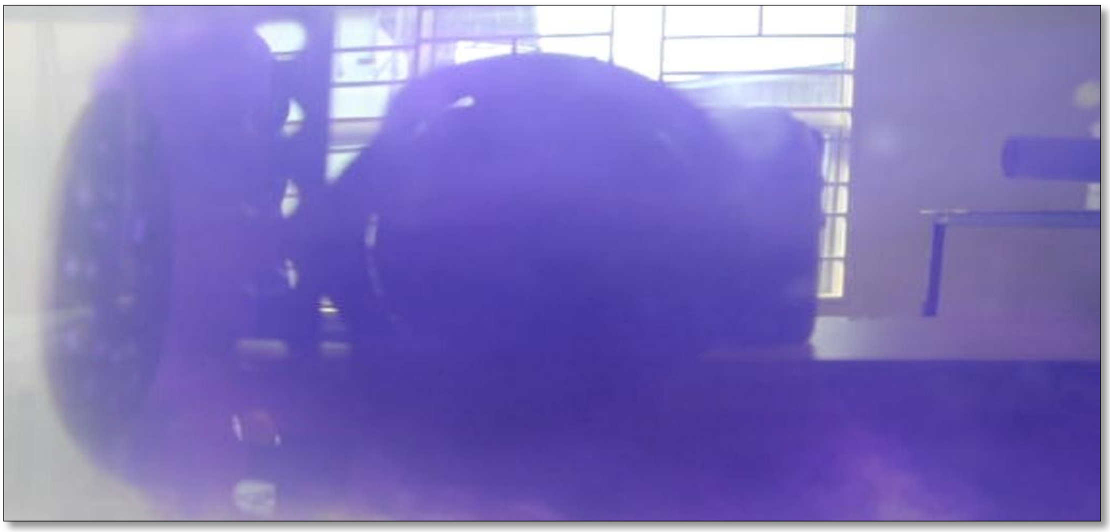

Figure 4.12: 14% wake effect experiment result.

Figure 4.13: 22% wake effect experiment result.

4.3 RESULT COMPARISON

Table 4.3: Comparison between numerical and experimental result

	Numerical		Experimental	
Disk porosity level	14%	22%	14%	22%
Coefficient of thrust (Ct)	2.0	1.12	2.2	1.35
Wake converging distance	4D	4D	4D	4D
Percent wake recovered	70%	67%	70%	70%

CHAPTER 5

CONCLUSION AND RECOMMENDATION

5.1 PROJECT CONCLUSION

It has been agreed that at 4D downstream, the wake effect is recovered around 70% for both numerical and experimental results.. The velocity at 4D downstream recovered 70% around 0.07 m/s compared to the velocity before the disk which is 0.1 m/s thus the kinetic energy of water are 70% restored. It can be concluded that the 10 m of tidal turbine with 1.12 to 2.2 thrust coefficient can be placed in the array of 40 m minimum distance between each other to have a 70% of wake recovery.

5.2 FURTHER RECOMMENDATION

5.2.1 Velocity Data Measurement Device

Most of the research related to this project use an advanced technology of velocity measurement such as acoustic doppler velocimeter (ADV) and pitot probe. The flowmeter use in this experiment occupies a 5 cm square of area thus decreasing the point of velocity which can be measured. The reading also gives a 2 decimal places and it is less accurate. Since the speed of velocity is slow, it is strongly recommended to use a more sensitive velocity measurement device.

5.2.2 Actuator Disk Adjustment

The actuator disk used is a manually own fabrication. The porosity of the disk can be increased if more experienced skill use to fabricate the disk. It is recommended that the disk is sent to a shop and fabricate thus increasing the porosity level with a finer surface. Furthermore the high porosity level will result in a low number of coefficients of thrust and can be manipulated to be as same as the first generation of marine current energy converter.

5.2.3 Load Cell

The use of load cell may improve the result since reference [33] state that the load cell is essential to measured the thrust coefficicent. Due to the unavailability of the load cell in the faculty, a strain gage is used.

5.2.4 Water Channel

The water channel design will improve the result by creating a similar water condition in a sea. Due to time and money constrain, the water channel may only support up to 20cm depth and 40cm long of steady flow water condition. A longer section of test channel may improve the result and gives a real distance the wake fully recovered.

LIST OF REFERENCES

1. Yun Seng Lim*, S.L.K., *Analytical assessments on the potential of harnessing tidal currents for electricity generation in Malaysia.* 2009.
2. Rosnazri Ali , Ismail Daut, Soib Taibb, *A review on existing and future energy sources for electrical power generation in Malaysia.* 2012.
3. report, C.T., *Uk, Europe and global tidal stream energy resource assesment.* 2005.
4. Bahaj, A.S., *Generating electricity from the oceans.* 2011.
5. X. Sun, J.P.C., I.G. Bryden, *Laboratory-scale simulation of energy extraction from tidal currents.* 2007.
6. Egbert GD, R.R., *Semi-diurnal and diurnal tidal dissipation from TOPEX/Poseidon altimetry. Geophysical Research Letters.* 2003.
7. K. Bilena, O. Ozyurta, K. Bakırcıa, S. Karslıb, S. Erdoganc, and O.C. M. Yılmaza, *Energy production, consumption, and environmental pollution for sustainable development: A case study in Turkey.* 2007.
8. *European Renewable Energy Council (EREC). Renewable energy target for Europe—20% by 2020.* 2005.
9. Watchorn M, T.T., Sayigh AAM, *Tidal stream renewable offshore power generation.* 2000.
10. Fergal O. Rourke *, F.B., Anthony Reynolds, *Marine current energy devices: Current status and possible future applications in Ireland.* 2009.
11. William D. Muir, J.G.W., *Improving connectivity between freshwater and marine environment for salmon migrating through the lower Snake and Columbia River hydropower system.* 2011.
12. Omar Yaakob, T.M.A.B.T.A.R., Mohamad Afifi Abdul Mukti, *Prospects for Ocean Energy in Malaysia.* 2006.
13. Sun, X., *Numerical and Experimental Investigation of Tidal Current Energy Extraction.* 2008.
14. *Ocean power: wave and tidal energy review.* 2004.
15. Haydar Faez Hassan n, A.E.-S., Othman A.Karim, *Tidal current turbines glance at the past and look into future prospects in Malaysia.* 2012.
16. *Lehigh University.Harnessing Tidal Energy:Barrages.*
17. *http://en.wikipedia.org/wiki/Rance_Tidal_Power_Station.*

18. Margaret Kadiri∗, R.A., Bettina Bockelmann-Evans, William Rauen, Roger Falconer, *A review of the potential water quality impacts of tidal renewable energy systems.* 2011.
19. S.M. Shafiea, T.M.I.M., b,∗, H.H. Masjukia, A. Andriyanaa, *Current energy usage and sustainable energy in Malaysia: A review.* 2011.
20. Koh SL, L.Y., *Preliminary investigation of the potential of harnessing tidal energy for electricity generation in Malaysia.* 2008.
21. Gómez, M.G., *MARINE CURRENT TURBINES: ARRAY EFFECTS.* 2008.
22. Leijon, M.G.U.L.a.M., *Ocean Energy.* 2005.
23. Alam, J., *Design and development of a marine current energy conversion system using hybrid vertical axis turbine.*
24. Ben Elghali, *Marine Tidal Current Electric Power Generation Technology: State of the Art and Current Status.* 2007.
25. *http://www.lunarenergy.co.uk/productOverview.htm.*
26. A.S Bahaj , L.E.M., M.D. Thomson, N. Jorge, *Characterising the wake of horizontal axis marine current turbines.* 2007.
27. A. Mason-Jones, D.M.D., C.E. Morris, T. O'Doherty, C.B. Byrne, *Non-dimensional scaling of tidal stream turbines.* 2012.
28. J.D. Anderson, J., *Governing Equations of Fluid Dynamics.*
29. Francesco Castellani , A.V., *An application of the actuator disc model for wind turbine wakes calculations.* 2012.
30. G. Crastoa*, A.R.G., F. Castellanib, E. Piccionib, *Wake modeling with the Actuator Disc concept.* 2012.
31. J. H. Ferziger and M. Peric, *Computational Methods for Fluid Dynamics.*
32. Luke Myers , B.B., Gregory Germain, Jack Giles, *Flow boundary interaction effects for marine current energy conversion devices.*
33. M. E. Harrison, W.M.J.B., L. E. Myers, A. S. Bahaj, *A comparison between CFD simulations and experiments for predicting the far wake of horizontal axis tidal turbines.* 2009.
34. Lim Yun Seng, K.S.L., *ANALYTICAL ASSESSMENTS ON THE POTENTIAL OF HARNESSING TIDAL CURRENTS FOR ELECTRICITY GENERATION IN MALAYSIA (http://www.utar.edu.my/contentRandD.jsp?YearArchive=2009&catid=9&contentid=417&2ndcontentid=1298).* 2009.